



## Information on Vinchucas and Chagas Disease

*Ils ne mouraient pas tous, mais tous étaient frappés.*

Les animaux malades de la peste.  
La Fontaine.

*Following a significant increase in the number of vinchucas observed at La Silla during the last summer, the Director-General of ESO asked Prof. Hugo Schenone, Director of the Department of Microbiology and Parasitology of the University of Chile to pay a visit to La Silla to investigate the situation. The following gives a summary of the resulting report.*

*What are vinchucas?* They are insects which belong to the "tratominos" group. Both the adult and the young of this species feed exclusively from the blood that they get by biting diverse animals such as mammals, birds and reptiles, including human beings.

*How do vinchucas reproduce and develop?* The pregnant females place their eggs, which are approximately 1.5 mm in length, in protected places. The young that come from the eggs are called nymphs. During the growth period, they change their skin until they reach the size of adults. The adults, which in general are winged, are egg-shaped, measure approximately 2 cm in length and are of black or dark brown colour. Their abdomens have yellowish or reddish spots in an alternation. The young or nymphs are either greyish or brown, the colour of earth.

*In which countries do vinchucas exist?* They exist in practically all countries of the American continent, except Canada.

*Are they the same kind in all these countries?* No. Numerous species exist, although some are common to several countries of the same region. In Chile only two types exist: a domestic

one called *Triatoma infestans* (lives in homes) and one living in the wild, called *Triatoma spinolai*. They have been found in rural regions between the latitudes 18° and 34° South.

*Do vinchucas carry any disease?* Yes, the so-called Chagas disease or American trypanosomosis.

*What is Chagas disease?* It is a parasitic infection produced by a protozoan called *Trypanosoma cruzi* which can be transmitted by infected vinchucas. The vinchuca does not inject the parasite when it bites, but on some occasions when the vinchuca has sucked much blood it may defecate and eliminate *T. cruzi* together with the defecation. This defecation, which appears like a dark coffee coloured liquid drop, may be clearly visible, and can contaminate either the wound made by the bite or small erosions of the skin caused by scratching, or it can fall directly into the ocular mucous membrane, thus starting the infection.

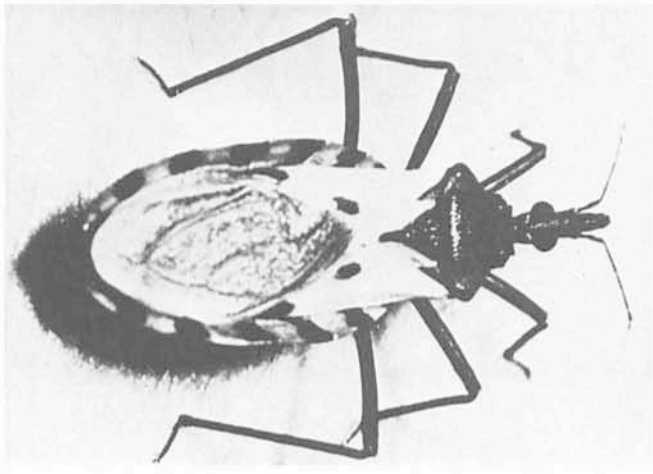
In the majority of cases, the vinchuca bite does not produce any infection, because not all vinchucas are infected, and it is necessary that they defecate at the moment of biting.

When infection occurs, after an incubation period without symptoms which lasts approximately ten days, symptoms may become evident that correspond to the acute phase of the illness which is characterized by swelling at the place of the bite where the parasite penetrated the skin, by fever, and by general malaise; very exceptionally one may suffer myocarditis and/or meningitis. After some weeks these symptoms diminish and may disappear, giving the impression of an apparent sudden cure of the infection.

Starting in the sixth month after the initial infection the illness enters its chronic phase which lasts during the whole life of the person and during which symptoms of myocardial effects, of the esophagus or the colon may appear.

In the majority of cases the infection shows no symptoms from the beginning.

*Can other animals be infected by the "Trypanosoma cruzi"?* Yes, specially the terrestrial mammals, wild and do-



One of the vinchucas that were sent to Europe for a test some years ago. Photographed by Dr. G. Schaub of the Zoological Institute of the Freiburg University (FRG).

mestic, which can be the source of infection of the domestic or wild vinchucas.

*Does any medical treatment exist for the Chagas disease?* Yes. At present two types of drugs exist, Nifurtimox and Benznidazol, both of proven efficiency.

*What is the situation at La Silla?* In this area the wild species *Triatoma spinolai* exists which, being attracted by the odor of humans, may bite them, especially during sleep.

The risk of infection for people is low, because only a very small percentage of infected vinchucas (6.5%) have been found, and moreover it is necessary that they defecate at the moment of biting.

*What precautions can be taken?* Use of protective screens against insects in the windows of the dormitories.

The ESO Administration is putting into practice a series of technical measures to control the vinchuca problem. In case a person is bitten, the appropriate blood test will be arranged. So far these tests have always had a negative result.

## Star Formation in Bok Globules

Bo Reipurth, Copenhagen University Observatory

### Introduction

Among the many dark clouds seen projected against the luminous band of the Milky Way are a number of small, isolated compact clouds, which often exhibit a large degree of regularity. These objects are today known as Bok globules, after the Dutch-American astronomer Bart Bok, who more than 30 years ago singled out the globules as a group of special interest among the dark clouds.

Bok globules usually have angular sizes of from a few arcminutes to about 20 arcminutes, with real sizes of typically 0.15 to 0.8 parsecs. It is generally not so easy to estimate the distance, and thus the dimensions, of a given globule. Most known globules are closer than 500 pc, since they normally are found by their obscuring effects, and more distant globules become less conspicuous because of foreground stars. A nearby, compact Bok globule is indeed a spectacular sight; when William Herschel for the first time saw a globule in his telescope, he exclaimed: "Mein Gott, da ist ein Loch im Himmel."

For many years the main tool to study globules were counts of background stars seen through the outer parts of the globules. When carefully and correctly executed, star counts can provide much valuable information; but with the advent of molecular radio astronomy it has now become possible to obtain precise data on masses, temperatures and composition of the globules. Typical globule masses are between  $15 M_{\odot}$  and  $60 M_{\odot}$ , and temperatures are around 10 K to 20 K. The interior of such a small, cold cloud is well protected against the more energetic radiation from stars, and so various atoms can combine to molecules, mainly of hydrogen, with important additions of carbon oxide, formaldehyde and many more exotic molecules.

Bok's conjecture in singling out the globules as a group was that, if stars (radius  $\sim 10^{11}$  cm, density  $\sim 1$  g/cm<sup>3</sup>) form out of denser regions in the interstellar medium (radius  $\sim 10^{19}$  cm, density  $\sim 10^{-22}$  g/cm<sup>3</sup>), then intermediate stages might be seen, representing proto-proto stars.

Subsequent observations have clearly shown that the main regions of star formation are not globules, but giant molecular

clouds, in which thousands of stars can form. Although globules thus are no longer necessary to understand the bulk of star formation in our galaxy, it is no less likely that a globule can form one or a few stars. The problem with this idea is just that no newborn stars had been found in association with a *bona fide* Bok globule.

### The Globules in the Gum Nebula

This situation has changed with the recent discovery of a large complex of globules in the Gum Nebula. The Gum Nebula is a huge, faintly luminous H II region spread over more than 30 degrees of the southern sky. At a distance of roughly 450 pc this corresponds to a radius of about 125 pc, making the Gum Nebula one of the largest structures known in our galaxy. Near its center are several objects which together produce the ultraviolet radiation that ionizes the gas in the nebula. Among these are Zeta Puppis, an extremely luminous O star with a mass of about  $100 M_{\odot}$ , Gamma Velorum, which is a massive binary system consisting of a Wolf-Rayet and an O component, as well as the Vela pulsar, a neutron star left over from a supernova explosion 10,000–20,000 years ago.

Pointing towards these objects are about 40 "windswept" or "cometary" globules, with sharp edges towards the center of the Gum Nebula, and several parsecs long, faintly luminous tails stretching in the opposite direction. This appearance can be understood as the eroding effect of the ultraviolet radiation from the luminous central stars, causing the globules to slowly evaporate and carrying material away from the dense globule heads. In this hostile environment most globules will be destroyed in a few million years. But this is long enough that stars can form in the denser globules.

### Bernes 135

Associated with one spectacular globule, CG 1, is a star, numbered 135 in a catalogue of nebulous stars by Bernes (Fig. 1). The diameter of CG 1 is 0.3 pc and its total length is 3.2 pc, and the mass of its dense head is probably of the order

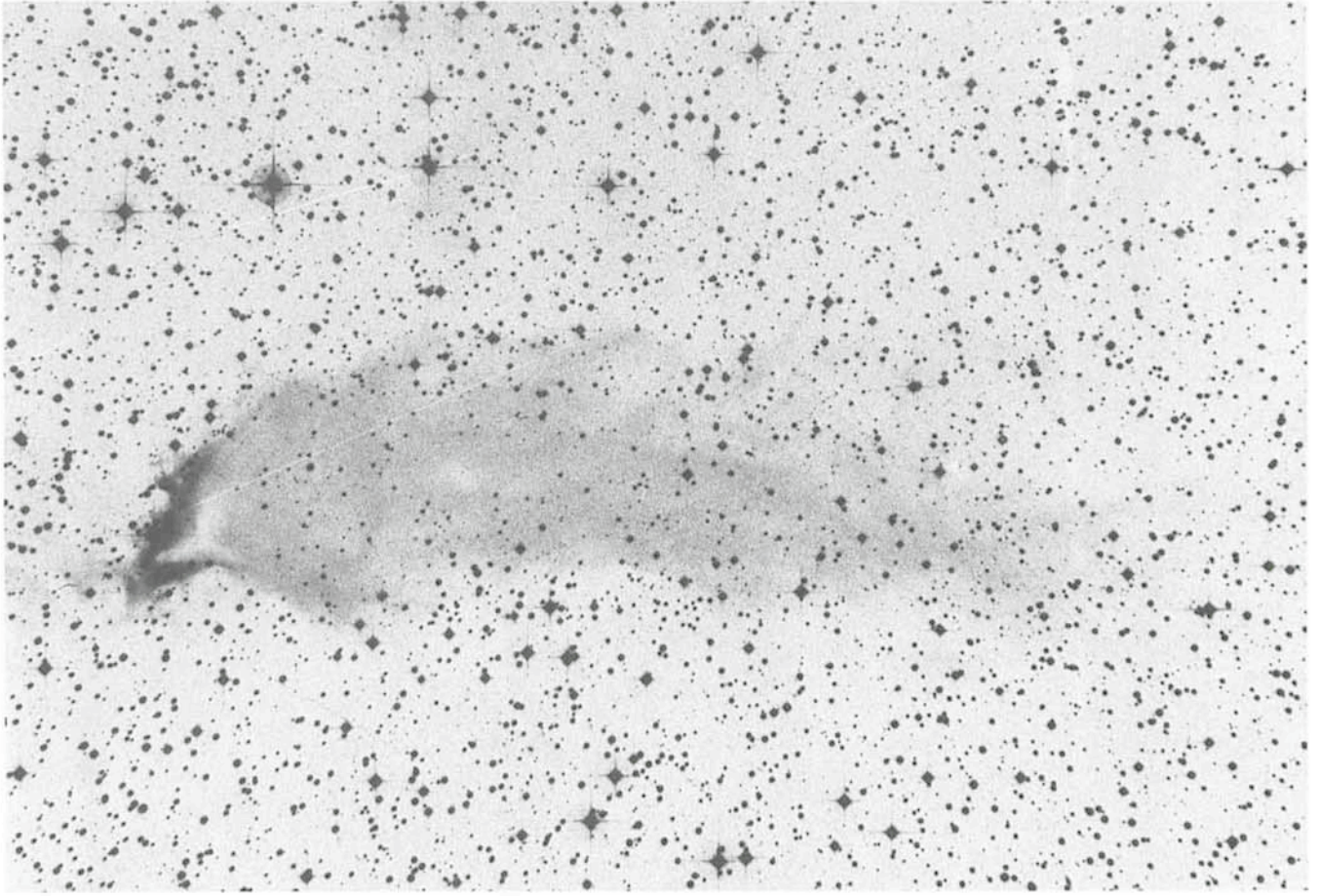


Fig. 1: The cometary globule CG 1 in the Gum Nebula. The length of the tail is over 3 pc. Very close to the dense globule head covered with bright rims is the young pre-main-sequence star Bernes 135 (SRC-J Schmidt plate).

of  $50 M_{\odot}$ . Could it be that Bernes 135 was born out of the globule?

A star is usually safely regarded as a pre-main-sequence star when it fulfils the following four conditions: (1) The star is associated with nebulosity and dark clouds, (2)  $H\alpha$  is seen in emission in its spectrum, (3) The star is weakly variable in an irregular manner, (4) The flux distribution of the star shows an infrared excess. All these criteria are fulfilled by Bernes 135. Observations with various telescopes on La Silla over the past two years have shown that Bernes 135 has a peculiar composite emission/absorption spectrum, which can be interpreted as an early F star surrounded by dense circumstellar material. Figure 2 shows a blue IDS spectrum from the ESO 3.6-m telescope of Bernes 135. It is noteworthy that the  $H\beta$  line at  $\lambda$  4861 has a central emission peak which is displaced bluewards, indicating outflow of matter with over 100 km/sec. Optical and infrared photometry shows that over 80% of the radiation from the star is being absorbed in this shell, which re-emits it as infrared radiation. Its visual magnitude varies by several tenths of a magnitude in an irregular manner on timescales of days, while its infrared magnitudes have been constant over nearly two years. The luminosity of Bernes 135 derived from the observations is almost  $50 L_{\odot}$ , and its effective temperature is about 6,800 K. Compared to theoretical calculations of the evolution of pre-main-sequence stars this suggests a mass of roughly  $2.5 M_{\odot}$ , a radius of about  $5 R_{\odot}$  and an age of about one million years.

The most common type of pre-main-sequence stars are the T Tauri stars, but the spectrum and the derived properties of Bernes 135 do not fit this group. Rather, it is hotter and more

luminous than these stars, and seems to belong to a part of the HR diagram in between the T Tauri stars and the Herbig Ae/Be stars. These stars are more massive young pre-main-se-

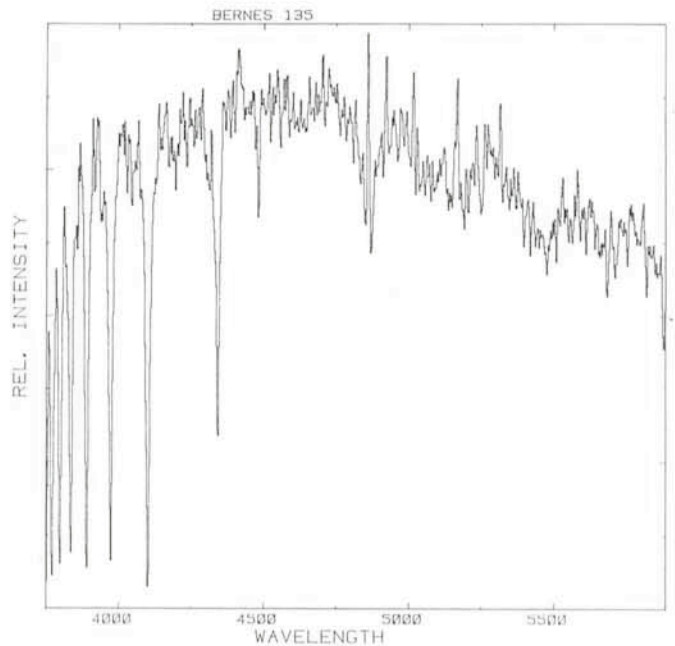


Fig. 2: Blue 114 Å/mm spectrum of Bernes 135, taken with the IDS on the 3.6-m telescope by Walter Eichendorf. The  $H\beta$  line at  $\lambda$  4861 shows a blueshifted central emission peak, indicating outflow of matter.

quence stars, and Figure 3 shows a HR diagram with a number of them plotted together with Bernes 135.

The association between a highly unusual young pre-main-sequence star and a dense Bok globule provides compelling evidence that Bok globules, at least under the proper circumstances, can indeed form stars. CG 1 may well be the smallest observed dark cloud known to have formed stars.

### Bok Globules and Herbig-Haro Objects

CG 1 is not the only one of the globules in the Gum Nebula which has formed stars, several of them are associated with stars and Herbig-Haro objects. Herbig-Haro objects are small nebulosities with peculiar forbidden emission-line spectra found in certain star-forming dark clouds. Often these objects are found close to a young star or an embedded infrared source, from which they move away with highly supersonic velocities. The Herbig-Haro objects may be associated with violent eruptions known to occur in some young stars.

An example of a Herbig-Haro object in one of the cometary globules in the Gum Nebula is seen in Figure 4. The Herbig-Haro object is the small oblong nebulosity near the center of one of the globules, numbered CG 30. This Herbig-Haro object is presently being studied by Pettersson and Westerlund, and its presence indicates that a young star is still embedded inside the globule.

Dark clouds are known to be inhomogeneous with "cores" of more dense material, and it is possible to understand the cometary globules in the Gum Nebula as such cores of dark clouds, exposed by the eroding effects of the ultraviolet radiation from the central O stars. Above the spectacular complex of globules in Figure 4 is seen a less dense, small dark cloud, an association known also for several others of the globules, and this can be understood as the remnants of the original cloud in which the core resided. In many cases, as in Figure 4, the globules show evidence of severe disruption, and this can be modelled using the theory of Rayleigh-Taylor and Kelvin-Helmholtz instabilities. The force involved is not radiation pressure, but the rocket effect, which arises when the ultraviolet radiation evaporates the outer layers of the globules, and the hot gas expands supersonically towards the O stars, pushing the globules away from the center of the Gum Nebula.

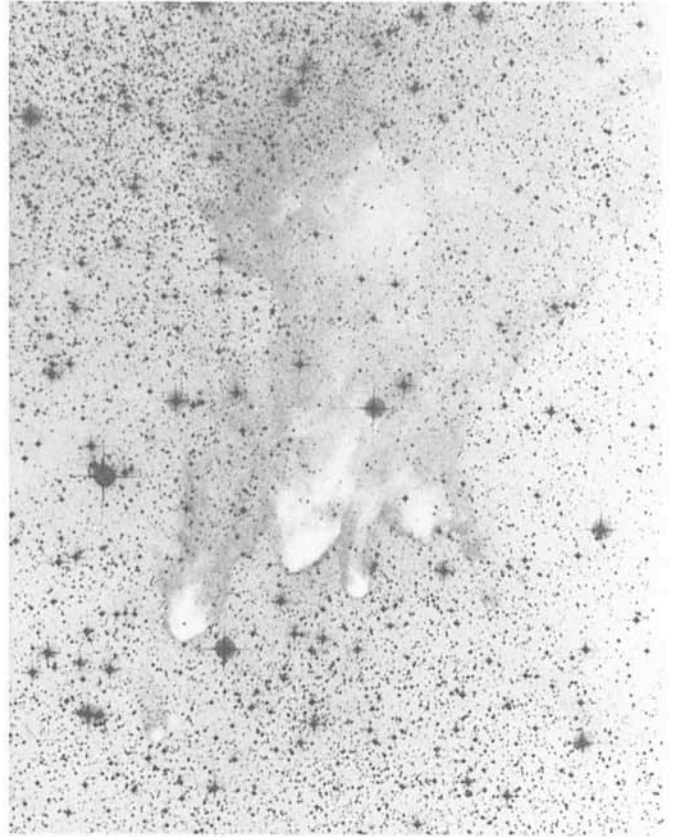


Fig. 4: The CG 30/31/38 complex of cometary globules in the Gum Nebula. The globules show evidence of disruption. A Herbig-Haro object is seen as a small nebulosity near the center of the globule CG 30 (SRC-J Schmidt plate).

Calculations using estimates of the amount of ultraviolet radiation available together with the above-mentioned principles show that the globules have existed for roughly a million years, in relatively good agreement with the present age of the O stars in the center of the Gum Nebula, as well as the age of Bernes 135.

In short, the present work has proven Bart Bok to be right in his idea that globules can form stars. It is suggested that Bok globules are cores from small molecular clouds, exposed after the ignition of massive O stars producing copious amounts of ultraviolet radiation in the region. After the stripping of the cores, they are partly compressed, partly disrupted, and this forces several of the globules into star-forming collapses. In some cases the more massive O stars will die before the globules have been destroyed, leaving isolated globules scattered along the plane of the galaxy, slowly expanding and dissolving into the interstellar medium.

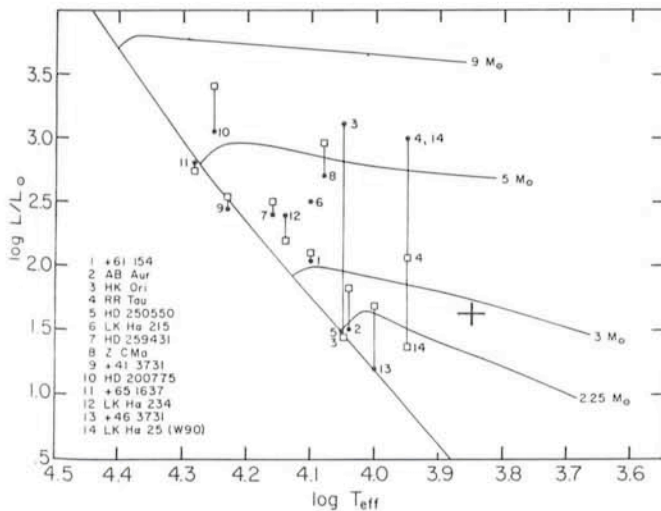


Fig. 3: The position of Bernes 135 (shown by a cross) in a theoretical HR diagram with a number of young Herbig Ae/Be stars. (Diagram from Strom, S. E., Strom, K. M., Yost, J., Carrasco, L. and Grasdalen, G.: Astrophysical Journal 173, 353, 1972.)

### ESO USERS MANUAL

A new version of the ESO Users Manual is now available. It has recently been distributed to astronomical institutes; if your institute has not received a copy, please contact the Visiting Astronomers Section, Garching. ESO urges all its users to read the manual carefully before applying for observing time.

The manual will be updated periodically and any errors that should be corrected or any information you would like to be included should be communicated to the editor, Anthony Danks.

# X-Ray Surveys with the Einstein Observatory

J. Danziger, ESO

## Introduction

Two different types of survey with the imaging instruments included in the Einstein Observatory are yielding results of particular interest in extragalactic astronomy and cosmology. The first is known as a "deep field" survey, and we will describe here the results for an observed region in Pavo. The second type is the "medium sensitivity survey" which attempts to identify a complete sample of faint X-ray sources (energy  $10^{-11.5}$  to  $10^{-13}$  ergs  $\text{cm}^{-2} \text{s}^{-1}$  in the 0.3–3.5 keV soft X-ray band) detected in the fields of previously known or studied X-ray sources. At present, the "medium sensitivity survey" is still being worked on and results are very preliminary.

## The Pavo Field

It was the purpose of the Pavo deep field survey (as well as those in Ursa Minor and Eridanus) described by Giacconi *et al.* (1979, *Ap. J.* **234**, L1) to detect all sources in a restricted field (40 arcminutes square) down to a limiting intensity of  $1.3 \times 10^{-14}$  ergs  $\text{cm}^{-2} \text{s}^{-1}$  in the energy range 1 to 3 keV. In this way one expected to resolve the diffuse X-ray background to this limit and then to identify optically these resolved sources. The Pavo field ( $21^{\text{h}} 10^{\text{m}}, -68^{\circ}$ ) was chosen because it is at high galactic latitude and contains no unusual optical or radio sources and no previously known X-ray sources. It was first observed with the IPC (Imaging Proportional Counter, whose spatial resolution is  $\sim 1$  arcminute) for 69,000 seconds, and subsequently 4 exposures were made with the HRI (High Resolution Imager whose spatial resolution is  $\sim 2$  arcseconds) with exposure times from 58,000 to 96,000 seconds. The IPC observation revealed 28 X-ray sources of which 22 were detected with the HRI. These 22 sources form the basis of the analysis discussed below.

Deep direct plates of the Pavo field were obtained in colours roughly equivalent to B and V, with the Anglo-Australian Telescope. Magnitudes of all objects, for which J ( $\sim$  B) was brighter than 23.8, were measured with COSMOS at the Royal Observatory Edinburgh. This process yielded 3,522 point sources (stars and quasars) and 1965 extended sources (galaxies) in the Pavo field. Of the 22 X-ray sources 3 show no optical counterpart in the error boxes, 14 have 1 image, 4 have 2 images and 1 has 3 images.

The number/J magnitude count for galaxies in Pavo is similar to that observed in other parts of the sky. Also the colour-magnitude diagram for stars is similar to other regions, in that one observes 2 populations of stars (or stellar objects); a red population extends redward from  $B-V \sim 1.6$  and fainter than  $B \sim 20$ , and a yellow population with approximately constant  $B-V \sim 0.6$  extends over a wide range of magnitude to the plate limit. The effect can be seen in Figure 1. This yellow population of stars is thought to be a halo population extending to 50 kpc from the Galaxy. The equivalent diagram for galaxies is shown in Figure 2.

Spectra of 9 candidate objects in 9 fields have yielded 4 quasars. These spectra of objects as faint as 20.7 were obtained with spectrographs on the AAT and the 3.6-m telescope at La Silla. Because of the low expected surface density of quasars we can say that these 4 identifications are virtually certain. The spectroscopy and direct plate material show that 4 galaxies and 3 stars are included in the candidate list. Because of the much higher surface density of stars and galaxies in this

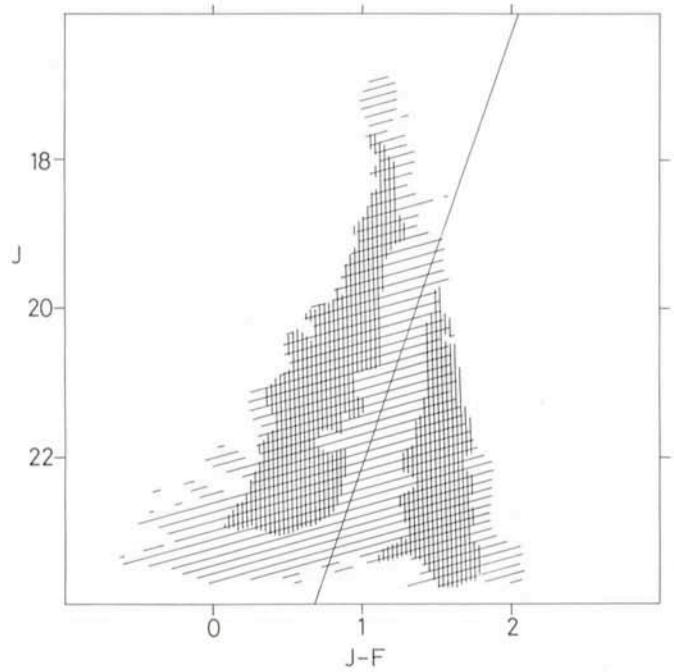


Fig. 1: Schematic colour-magnitude diagram for point sources in the Pavo field. The shading is intended to convey an idea of the density of points in this graph.  $J-F$  is roughly equivalent to  $B-V$ .

field, the presence of these 7 objects is consistent with chance coincidences with the X-ray error boxes.

We noted above that 3 X-ray sources had no optical counterparts and 4 have certain identifications as quasars. It is therefore the nature of the remaining 15 identifications that is crucial to

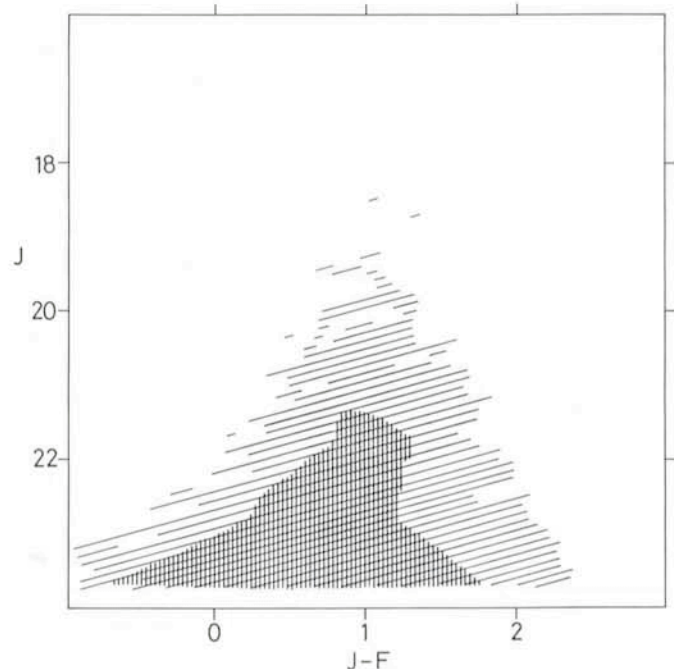


Fig. 2: Schematic colour-magnitude diagram for extended sources in the Pavo field.

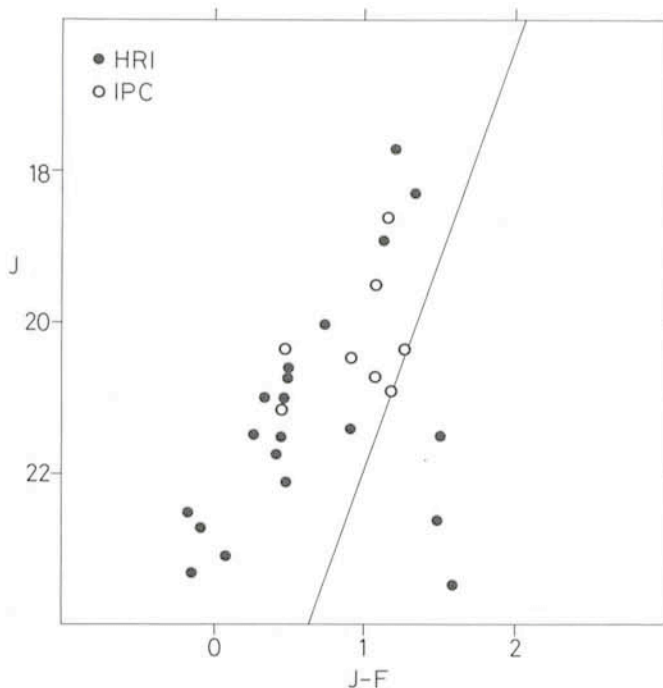


Fig. 3: Colour-magnitude diagram for selected X-ray point sources in the Pavo field.

our understanding of the source content. Unfortunately 13 of these X-ray sources have candidates in the error boxes 21 magnitude or fainter, which are at present beyond the reach of currently available spectroscopic equipment in the southern hemisphere. One is therefore forced to resort to statistical arguments to make further progress.

A statistical test comparing the proportion of red and yellow stars in the X-ray candidates and in the field stars shows that a much higher proportion of the X-ray candidates belongs to the yellow population. However, because we have only 17 stellar objects as candidates in the yellow population, we cannot conclude that the number-magnitude relationship is significantly different from that found for the yellow field stars. One sees this effect in Figure 3. Thus far, one has shown only that a reasonably high proportion of these candidates *could* be quasars. The statistics of small numbers does not preclude the possibility that a reasonably high number could be galactic stars. One can argue that number counts for all quasars provide sufficient objects to account for all the X-ray candidates. This is a necessary but not sufficient condition in this statistical approach, since there are also enough yellow field stars to do the same trick! Similarly, an argument based on the ratio of X-ray to optical luminosity of the candidates is only strong enough to be consistent with their being quasars, but does not rule out yellow stars as possible sources. One has noted also that the average colour of the candidates is bluer than the average colour of the yellow field stars. Even if this is a statistically significant result, it is premature to draw strong conclusions from it without knowing what the average colour of faint X-ray stars might be. Finally, one should not overlook the fact that Warwick *et al.* (*Monthly Notices of the Royal Astronomical Society* **190**, 243, 1980) have observed a 2.5 to 7.2 per cent anisotropy in the X-ray background which is consistent with galactic stars in an extended halo providing a considerable proportion of the candidates.

Radio observations at 6 cm with the Parkes 64-m telescope detected only one source associated with the X-ray identifications. This was one of the four quasars and it has an inverted

spectrum. Thus no unusual radio properties have been observed.

It is now apparent that use of the Pavo deep field survey to settle questions of the X-ray background requires more detailed knowledge of 12 to 14 candidates for which spectra are lacking. Until the Space Telescope is in operation the best possibility for achieving this seems to be multi-colour observations with broad or intermediate band filters capable of distinguishing quasars from stars, and a sensitive linear detector.

## The Medium Survey

At this stage the optical observations and analysis of sources detected in the medium survey are continuing, and may eventually lead to stronger conclusions than the deep field surveys have provided. When all the results are combined there should be well over 100 source identifications from both hemispheres to be discussed and evaluated. In the meantime a zoo of interesting identifications is expanding. Members of this zoo include quasars, Seyfert galaxies, clusters of galaxies, BL Lac objects and stars.

Only one BL Lac object has been found in an optical identification programme for a complete sample of *faint* X-ray sources. Since this one object represents 2 per cent of the total content, which is less than the 7 per cent content found for brighter X-ray sources, one can say that BL Lac objects do not evolve similarly to quasars and Seyfert galaxies! These latter objects change their contribution from 41 to 74 per cent over the same range of decrease of X-ray flux. Given this trend it seems probable that BL Lac objects do not contribute significantly to the soft X-ray background. Their evolutionary trend is rather similar to that shown by clusters of galaxies, where only weak cosmological evolution is apparent.

The work described in a qualitative way above results from collaborations with various combinations of the following astronomers: R. E. Griffiths, J. Bechtold, R. Giacconi, S. S. Murray, P. Murdin, M. Smith, H. McGillivray, M. Ward, J. Lub, B. Peterson, A. Wright, M. Batty, D. Jauncey, D. Malin, J. Stocke, J. Liebert, H. Stockman, T. Maccacaro, D. Kunth, H. de Ruiter.

## List of Preprints Published at ESO Scientific Group

September – November 1981

169. E. A. Valentijn and R. Giovanelli: 21 cm Line Observations of cD Galaxies. *Astronomy and Astrophysics*. September 1981.
170. A. C. Danks: A Carbon Star in the Globular Cluster Lindsay 102. *Astronomy and Astrophysics*. September 1981.
171. G. F. Gahm and J. Krautter: On the Absence of Coronal Line Emission from Orion Population Stars. *Astronomy and Astrophysics*. September 1981.
172. E. A. Valentijn: The 1919 + 479 Radio Tail, a Moving Galaxy within an Accumulated Gaseous Halo. Proc. IAU Symp. No. 97 "Extragalactic Radio Sources". September 1981.
173. P. A. Shaver: The Radio Morphology of Supernova Remnants. *Astronomy and Astrophysics*. November 1981.
174. A. Sandage and G. A. Tammann: Steps toward the Hubble Constant VIII. The Global Value. *Astrophysical Journal*. November 1981.
175. S. D'Odorico and M. Rosa: Wolf-Rayet Stars in Extragalactic H II Regions: Discovery of a Peculiar WR in IC 1613/#3. *Astronomy and Astrophysics*. November 1981.
176. K. R. Anantharamaiah, V. Radhakrishnan and P. A. Shaver: On the Statistics of Galactic H I Clouds. Proc. 2nd Asian-Pacific Regional Meeting of the IAU, Bandung, Indonesia, Aug. 24–29, 1981. November 1981.

# The “Continuous” Central Stars of Planetary Nebulae – Are their Spectra Really Continuous?

R. P. Kudritzki and K. P. Simon, *Institut für Theoretische Physik und Sternwarte der Universität Kiel*

R. H. Méndez, *Instituto de Astronomía y Física del Espacio, Buenos Aires*

## The Puzzle of the “Continuous” Central Stars

Twenty-five per cent of all central stars of planetary nebulae which have been studied spectroscopically are classified as “continuous”, which means that they do not show any sign of stellar absorption or emission lines, at least in the visible part of the spectrum. The existence of this kind of spectrum poses an interesting problem: The effective temperatures of the “continuous” objects can be estimated from the emission line spectrum of the surrounding nebula by means of the well-known “Zanstra method”. As it turns out, the temperatures are mainly between 50,000 K and 100,000 K. On the other hand, non-LTE model atmosphere calculations for very hot stars (as carried out in Kiel) show that even at 100,000 K there should be easily detectable H or He lines for any reasonable surface gravity, unless the atmosphere is essentially free of these elements. But even if we admit the absence of hydrogen and helium, we can estimate that strong lines of carbon (or nitrogen or oxygen) should be observable in this case.

## A Solution?

A way out of this problem is an idea first published by Aller (1968, 1976), who stated that probably many of the “continuous” CPN have weak, narrow absorption lines which are completely masked by overlying nebular emissions. However, he also mentioned that there are at least a few “bright” stars which, even at coudé dispersions, did not exhibit stellar lines and which therefore have to be regarded as true examples of the “continuous” spectral type: NGC 3242, NGC 7009, NGC 7662.

Despite of the negative result for these three stars, Aller’s idea still remained attractive for us. The main reason for this was a diagram which is shown in Figure 1. In this diagram the surface brightness of the surrounding nebula (in units of the stellar flux in the V-band) is plotted versus the apparent magnitude of the central star. We divided the central stars into three spectroscopic classes: objects with absorption lines (O, sdO, Of), objects with broad stellar emission lines (OVI, WR) and the “continuous” objects. The diagram is striking: absorption-line objects are placed in nebulae with relatively low surface brightness: The fainter the central star, the weaker the nebular surface brightness. This is obviously a selection effect, caused by the fact that, at the low resolution necessary for faint objects, the surface brightness has to be very low to make stellar absorption features detectable. On the other hand, the “continuous” objects are embedded in nebulae with relatively high surface brightness. This means that, if these stars have stellar absorptions, there is a good chance that they are masked by nebular emissions.

Also the emission-line objects are mainly found within nebulae of high surface brightness. However, in this case the stellar emission lines are very broad (Aller, 1968, 1976), so that the presence of strong nebular lines does not affect the identification of these spectral types.

## An IDS Spectrum of NGC 3242

From Figure 1 we concluded that “continuous” central stars are probably rather similar to the absorption-line objects, but that in this case strong nebular emission lines fill in the photospheric absorptions. We, therefore, concentrated on those objects which are close to the border between “absorption line” and “continuous” CPN. One of these objects is NGC 3242: We observed this central star on December 8/9, 1980 with the Image Dissector Scanner and the Boller and Chivens spectrograph at the Cassegrain focus of the ESO 3.6-m telescope. We used a grating of 1,200 grooves  $\text{mm}^{-1}$ , giving a dispersion of 29  $\text{\AA}/\text{mm}$  in the 2nd order. To reduce the contribution of the nebular light as far as possible without losing to much stellar light we selected an entrance aperture of  $2 \times 2$  arcseconds in size.

Figure 2 shows the spectrum of the central star of NGC 3242 from 4220 to 4780  $\text{\AA}$ . It is flat field corrected and wavelength calibrated by means of a He-Ar comparison spectrum taken before and after observation of the star. Besides the typical nebular emissions ( $\text{H}\gamma$ ,  $[\text{O III}] \lambda 4363$ ,  $\text{He I} \lambda 4471$ ,  $[\text{N III}] \lambda 4634$ ,  $\lambda 4641$ ,  $\text{C IV} \lambda 4658$ ,  $\text{He II} \lambda 4686$ ,  $[\text{Ar IV}] \lambda 4712$ ,

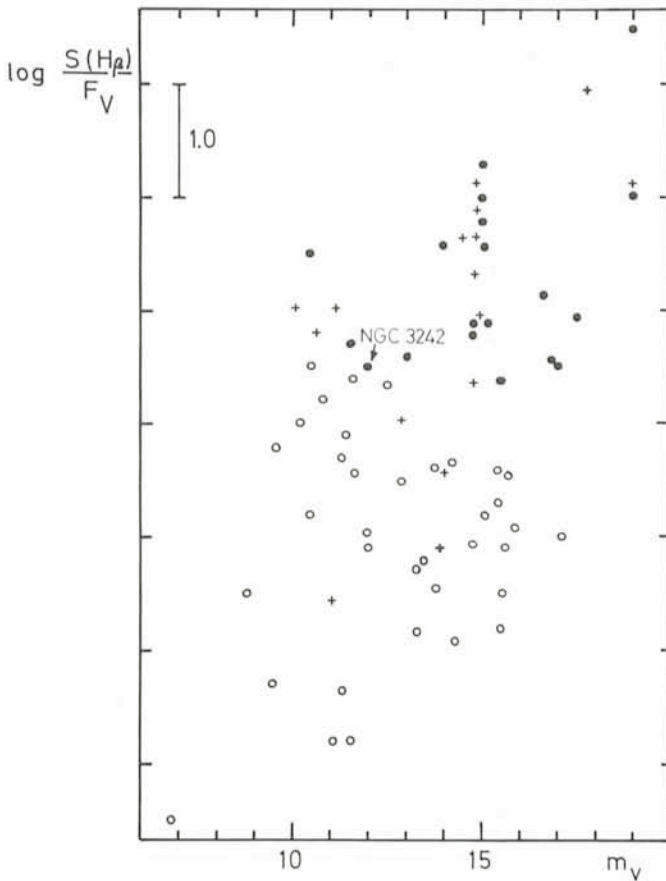


Fig. 1: The surface brightness of planetary nebulae  $S(\text{H}\beta)$  (in units of the stellar flux  $F_V$ ) versus apparent magnitude  $m_V$  of the central stars. The central stars are divided into three classes: + objects with broad emission lines (WR, OVI), o absorption line objects (sdO, O, Of), ● continuous objects. The position of NGC 3242 is also indicated. For discussion see text.

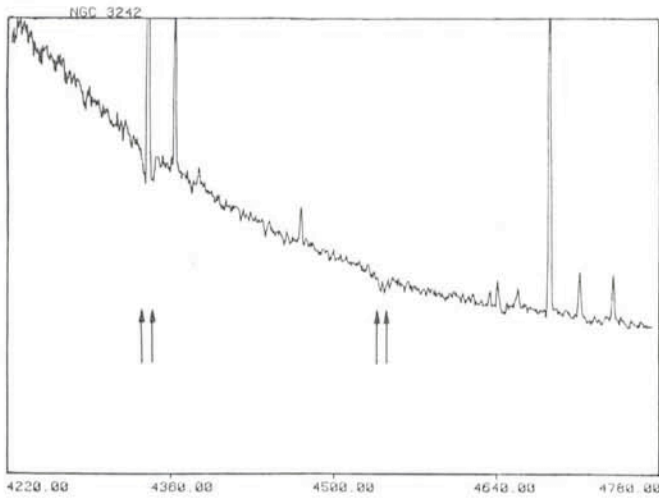


Fig. 2: IDS spectrum of NGC 3242. The photospheric absorption of  $H\gamma$  and He II 4542 are indicated by arrows. The abscissa refers to wavelengths in Angström. The intensity scale is in arbitrary units, the bottom corresponds to zero intensity.

$\lambda$  4740) we find quite normal photospheric absorptions at  $H\gamma$  and He II 4542 (see also Kudritzki *et al.*, 1981). Obviously, our observation reveals that one of the best examples among "continuous" central stars is a normal absorption-line object.

One might ask why the absorption lines in the spectrum of NGC 3242 have not been discovered before: notice that the resolution of our spectrum (FW HM  $\approx 1.6$  Å) should be lower than that of Aller's coude spectrograms. On the other hand, our IDS observations have three advantages:

- (a) A small entrance aperture, which reduces the contribution from the strong nebular emissions, thus permitting to look deeper into the absorption line cores.
- (b) A much better signal-to-noise ratio, which helps detection of low-contrast absorption features.
- (c) The linearity of the detector, which allows to get rid of all the well-known photographic effects, which occur at the junction of dark and bright areas.

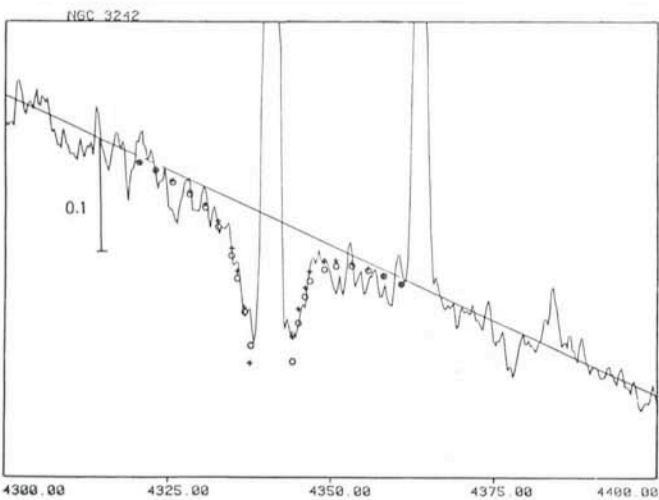


Fig. 3: Intensity tracing around  $H\gamma$  compared with non-LTE profiles calculated for  $T_{\text{eff}} = 50,000$  K,  $\log g = 4.0$  (crosses),  $T_{\text{eff}} = 100,000$  K,  $\log g = 5.0$  (circles) and  $y = N(\text{He})/N(\text{He}) + N(\text{H}) = 0.09$ . The calculations are convolved with the instrumental profile. Furthermore, the blending with the corresponding He II line has been taken into account, which causes the slight asymmetry in the theoretical profile. 10% below continuum intensity is indicated by the bar.

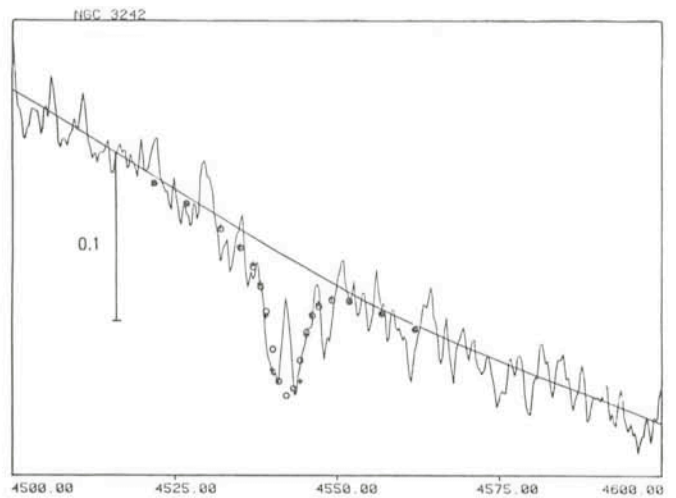


Fig. 4: Intensity tracing around He II 4542 compared with the non-LTE profiles for  $T_{\text{eff}} = 50,000$  K,  $\log g = 4.0$ ,  $y = 0.09$  (crosses) and  $T_{\text{eff}} = 100,000$  K,  $\log g = 5.0$ ,  $y = 0.09$  (circles).

## A Comparison with Non-LTE Model Atmosphere Calculations

The  $H\gamma$  and He II 4542 absorptions can be used for an estimate of surface temperature, gravity and helium abundance of NGC 3242. This can be done by a comparison of the observed profiles with the results of non-LTE model atmosphere and line formation calculations (see Hunger and Kudritzki, 1981, *Messenger* No. 24, page 7, Kudritzki and Simon, 1978, or Méndez *et al.* 1981).

Since in the case of NGC 3242 only two absorption lines can be used for a fit, whose cores, additionally, are contaminated by nebular emission, the result is a bit uncertain. We find that the star has a normal helium abundance (i.e.  $N_{\text{He}}/(N_{\text{H}} + N_{\text{He}}) = 9\%$ ) and a temperature between 100,000 K and 50,000 K. The gravity is between  $\log g = 4.0$  or 5.0. This is demonstrated by Figures 3 and 4, which show that the observed profiles can be

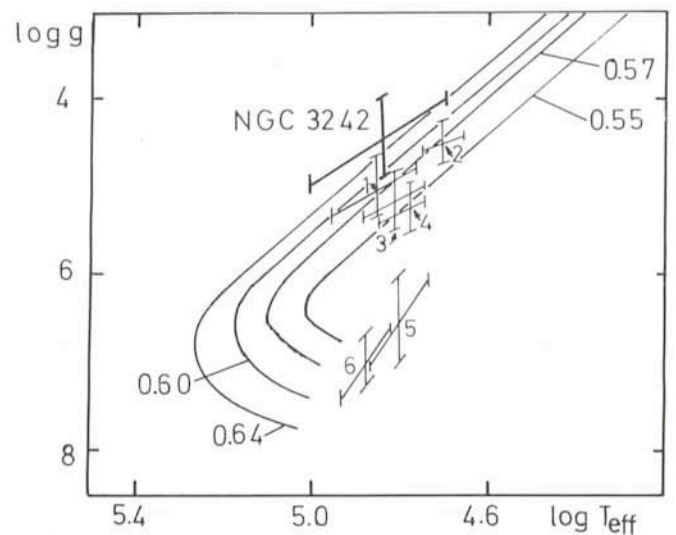


Fig. 5: Locus of NGC 3242 in the  $(\log g, \log T_{\text{eff}})$ -plane compared with 6 other CPN (Méndez *et al.*, 1981) and evolutionary tracks descending from the AGB as calculated by Schönberner (1979, 1981). The numbers designating the tracks refer to masses in solar units. The six other CPN's are: 1: NGC 4361; 2: NGC 1535; 3: A 36; 4: NGC 1360; 5: NGC 7293; 6: A 7.

fitted at  $T_{\text{eff}} = 100,000$  K,  $\log g = 5.0$  and  $T_{\text{eff}} = 50,000$  K,  $\log g = 4.0$ , if a normal helium abundance is assumed.

In spite of these uncertainties, the locus of NGC 3242 in the ( $\log g$ ,  $\log T_{\text{eff}}$ )-plane, obtained from the comparison with non-LTE calculations, contains some additional information about the nature of the star. In Figure 5 the position of the star is shown, together with six absorption line central stars which have been analysed already before (Méndez *et al.*, 1981) and with theoretical evolutionary tracks computed by Schönberner (1979, 1981) (see also Hunger and Kudritzki, 1981, *Messenger*, No. 24, page 7). If we assume that these tracks represent the evolution of all the PN central stars shown here,

we can conclude that NGC 3242 is slightly more massive than the other objects, which have masses from  $0.6 M_{\odot}$  to  $0.55 M_{\odot}$ .

## References

- Aller, L. H.: 1968, IAU Symp. 34, eds. Osterbrock and O'Dell, page 339.  
 Aller, L. H.: 1976, *Mem. Soc. Roy. Sci. Liège*, 6<sup>e</sup> série, IX, p. 271.  
 Kudritzki, R. P., Simon, K. P.: 1978, *Astron. Astrophys.* **70**, 653.  
 Kudritzki, R. P., Méndez, R. H., Simon, K. P.: 1981, *Astron. Astrophys.* **99**, L 15.  
 Méndez, R. H., Kudritzki, R. P., Gruschinske, J., Simon, K. P.: 1981, *Astron. Astrophys.* **101**, 323.  
 Schönberner, D.: 1979, *Astron. Astrophys.* **79**, 108.  
 Schönberner, D.: 1981 *Astron. Astrophys.*, in press.

# Variability of the Continuum and the Emission Lines in the Seyfert Galaxy Arakelian 120

K. J. Fricke and W. Kollatschny, *Universitäts-Sternwarte Göttingen*

## Introduction

The brightness variability of Seyfert galaxies and quasars is one of the most direct pieces of evidence for the intrinsic smallness of the optical continuum source in these objects. If the power of a source varies with a time scale  $\tau$  by a significant amount it must originate from a region which cannot have a size much larger than  $c \cdot \tau$  across where  $c$  is the velocity of light;  $\tau$  is observed to be typically of the order of months for such sources but may be much less. Not only the continuum strength but also the emission lines may vary in strength and shapes. This phenomenon is interesting with regard to the structure and kinematics of the line-emitting region as well as to the radiation mechanism within the continuum source.

A schematic sketch of an active galactic nucleus is shown in Figure 1. A nucleus of a Seyfert 1 galaxy or of a quasar consists of three components: (i) the optically unresolved (i. e. smaller than  $\sim 1$  arcsec) continuum source which emits predominantly radiation exhibiting a nonthermal spectrum; (ii) a small inner region ( $\sim 0.1$ – $1.0$  pc) from which the broad hydrogen and "permitted" lines originate with equivalent velocity dispersions typically 3,000 km/s up to 10,000 km/s and beyond. The electron density in the emitting clouds must in this region be larger than  $10^6 \text{ cm}^{-3}$  and may range up to  $10^{11} \text{ cm}^{-3}$ . In the latter case electron scattering may account for the full width of the permitted emission lines. Synthetic integrated line profiles for such a cloud aggregate show that the total number of these clouds must be enormous (E. Capiotti *et al.*, 1981, *Astrophysical Journal* **245**, 396); it has been estimated to be as large as  $10^{11}$  from observations (1981, H. Netzer, Proc. of the 5th Göttingen-Jerusalem Symposium, Göttingen 1980). A very clumpy structure has also been postulated on theoretical grounds (G. R. Blumenthal and W. G. Mathews, 1979, *Astrophys. J.*, **233**, 479). The total mass of the clouds is relatively small ( $\leq 1,000 M_{\odot}$ ). This region is probably entirely absent in the so-called Seyfert 2 galaxies; (iii) an outer region from which the narrow "forbidden" lines like the nebular line of  $\text{O}^{++}$  originate and which is  $\sim 500$  pc across.

There is evidence that the radiation from at least the inner regions (i) and (ii) may vary. We report in this article on continuum and spectrum variations in the Seyfert 1 galaxy Arakelian 120 which we observed in the optical with the ESO 3.6-m and 1.5-m telescopes and in the UV using the IUE telescope operated from Villafraanca near Madrid.

Long-term optical variability of Akn 120 since 1929 has been established by Miller from the University of Georgia, Atlanta, who inspected archival plates of the Harvard College Observatory. In addition, he reported rapid variability during the epoch 1977–78 with amplitudes  $\sim 0.3$  mag on a time scale of  $\sim 1$  month which confirms earlier work by Lyutyi from the Soviet Union. Variability of this source on somewhat longer time scales ( $\leq 1$  year) are also known from radio and X-ray measurements.

## Continuum Variations

We first observed Akn 120 in October/November 1979 in the optical and UV (for observational details see an article by H.

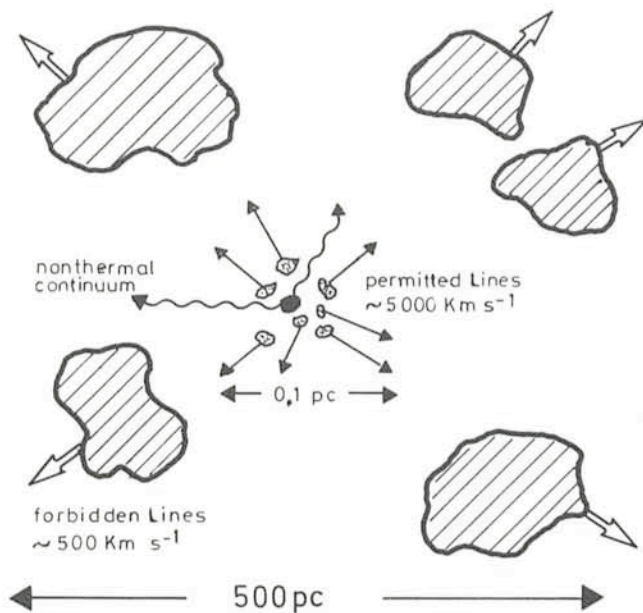


Fig. 1: Schematic model for a Seyfert 1 nucleus with its three components: (i) a point-like central source of nonthermal continuum radiation, (ii) a broad emission line region  $\leq 1$  light-year across with numerous fast moving dense ( $n_e > 10^6 \text{ cm}^{-3}$ ) clouds emitting the permitted lines, and (iii) a narrow emission line region  $\sim 500$  pc across containing less dense ( $n_e \leq 10^5 \text{ cm}^{-3}$ ) clouds with smaller velocities.

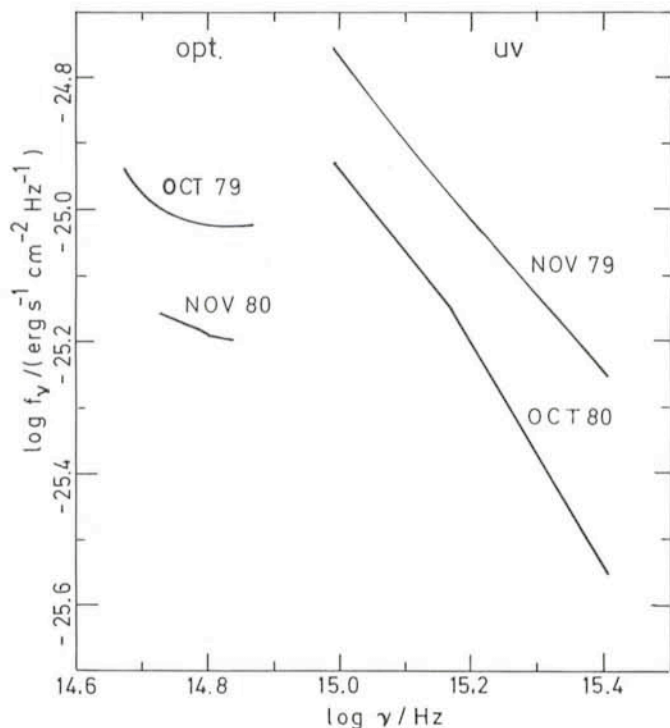


Fig. 2: The optical and UV continuum flux distributions for Akn 120 at two epochs.

Schleicher and H. W. Yorke in the *Messenger* No. 22). We found in this source an unusually high  $\text{Ly}\alpha/\text{H}\beta$  ratio, very strong UV Fe II emission and a jump of the continuum between 3000 and 4000 Å, a phenomenon which already was known from some other sources. We then re-observed Akn 120, again nearly simultaneously, in the optical and UV, a year later. Figure 2 shows for both epochs the optical and the UV continua. At the second epoch the continuum emission had dropped by a factor  $\sim 1.5$ , everywhere conserving the strength of the jump between the UV and optical portions of the continuous spectrum.

### Emission-Line Variations

The absolute intensities of all emission lines varied not more than by a factor of 2 and in the same direction as the continuum.

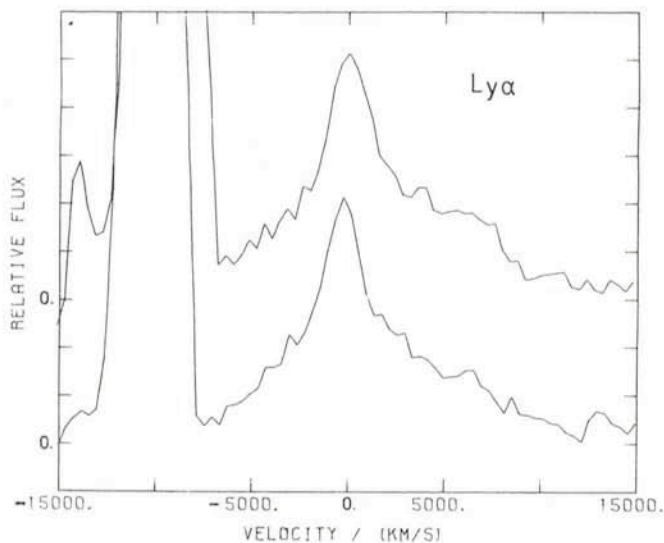


Fig. 3:  $\text{Ly}\alpha$  profiles of Akn 120 at two epochs (Nov. 1979 lower profile; Oct. 80 upper profile) normalized to their peak intensities.

$\text{Ly}\alpha$  and  $\text{H}\beta$  changed in absolute strength approximately proportional to the continuum, i.e. their equivalent widths stayed nearly constant. The line profiles, however, varied markedly and in a different fashion from line to line. This is apparent from Figures 3 and 4 where the  $\text{Ly}\alpha$  and  $\text{H}\beta$  profiles are compared for both epochs. The variations in the relative profile of  $\text{Ly}\alpha$  are only slight but clearly visible. The  $\text{H}\beta$  profile on the other hand developed a pronounced double-horn structure through a relative enhancement of its red wing. Such variations in the  $\text{H}\beta$  profile had not been observed during the previous years from 1974–79 in spite of the detection of continuum variability during this time. A detailed description of the line and continuum variations is contained in a forthcoming paper (Kollatschny, Schleicher, Fricke and Yorke, 1981, *Astronomy and Astrophysics*, in press). Variations of the Balmer line profiles at different epochs have independently been observed by C. B. Foltz and B. M. Peterson of the Ohio State University.

### Conclusions

The parallel variation of the broad components of the hydrogen lines and of the continuum with the equivalent widths remaining nearly constant is consistent with the picture that the broad emission (cf. Fig. 1) is confined to a spatial region less than a light-year across, since only then a variability in the ionizing continuum flux is propagated fast enough to the emitting cloudlets in this region.

The explanation of the different behaviour of the shapes of  $\text{Ly}\alpha$  and  $\text{H}\beta$  is not straightforward. It probably indicates that these lines originate from different locations in the emitting clouds. The change of a line profile as such may be due to a time variation in the spatial distribution of the ensemble of clouds emitting the broad lines; this in turn might be caused by large-scale instabilities or by coalescence of clouds. Alternatively, partial obscurations of this region by surrounding absorbing clouds may cause observed phenomena like the disappearance and reoccurrence of emission in the line wings.

Presumably, it is a long way from now until a detailed explanation of such line variations can be given. Parametrized calculations in terms of the multi-cloud model for the broad line region, adopting a flattened and inclined cloud distribution, are presently being done by us and hopefully will prove useful.

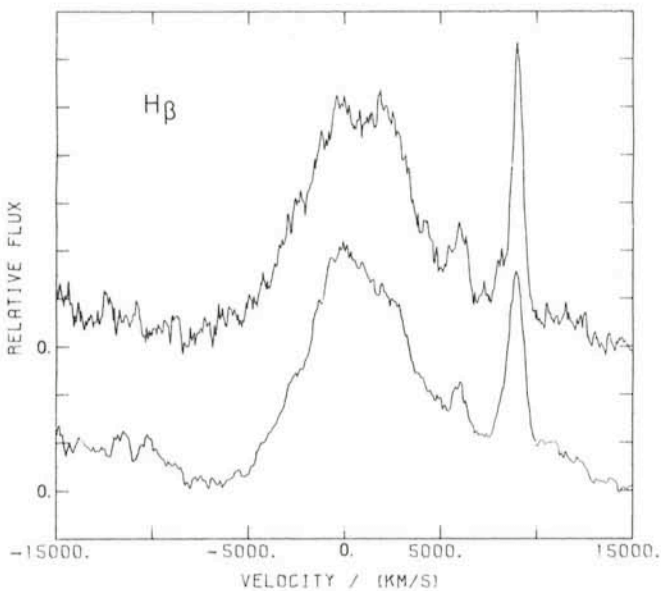


Fig. 4:  $\text{H}\beta$  profiles of Akn 120 at two epochs (Oct. 1979 lower profile; Nov. 80 upper profile) normalized to their peak intensities.

Akn 120 is certainly an excellent object for optical photometric and spectroscopic monitoring. It also recommends itself for long-term observations in the radio, infrared and X-ray spatial regions.

## Acknowledgements

This work was in part made possible by a grant (Fr 325/8 and Fr 325/12) of the Deutsche Forschungsgemeinschaft.

Announcement

## SECOND ESO INFRARED WORKSHOP

19–22 April 1982

*Organizing Committee:* R. van Duinen (Groningen), M. Grewing (Tübingen), A. Moorwood (ESO, Chairman), P. Salinari (Florence), F. Sibille (Lyon).

This Workshop is being organized with the aims of reviewing the status and performance of the many infrared groundbased facilities and instruments which have come into operation since the last ESO Infrared Workshop in Sweden in 1978 and to promote discussion on three topics of interest for the future:

- the infrared astronomical requirements of future Very Large Telescopes on the ground,
- the areas in which groundbased and airborne observations can best complement future space missions,
- the use of array detectors and the possible spin-offs to be expected from infrared space technology in groundbased and airborne instrumentation.

An exchange of views in these particular areas is considered to be timely bearing in mind ESO's on-going VLT studies, the imminence of the IRAS launch, the advanced technical state of the

GIRL Spacelab project and the widespread interest being displayed in a European Astroplane and ESA's study of an Infrared Space Observatory.

The meeting will be organized around invited reviews of the major projects plus contributions, submitted in response to this announcement, on the capabilities of current instruments and techniques, detector and instrumental developments. In keeping with the desired Workshop atmosphere, however, we intend to devote considerable time to discussion and will particularly welcome contributors interested in expressing their ideas and prejudices on the above themes.

It is hoped that the results will be suitable for publication by ESO. Attendance will have to be limited to around 70.

Further information and application forms can be obtained by contacting

Dr. A. F. M. Moorwood  
Infrared Workshop  
ESO  
Karl-Schwarzschild-Str. 2  
D-8046 Garching bei München  
Federal Republic of Germany

## Observations of the Giant Bubbles in the Large Magellanic Cloud

*Y. and Y. Georgelin, A. Laval, Observatoire de Marseille  
G. Monnet, Observatoire de Lyon  
M. Rosado, Instituto de Astronomía (Mexico)*

### Introduction

Deep monochromatic photographs through narrow-band interference filters on nearby spiral galaxies reveal large numbers (50–100) of circular shaped H II regions, with usually weak or absent central emission. They are called by various names; arcs, loops, rings, shells, etc. . . ., and are clearly the two-dimensional projections of more or less spherical bubbles of ionized gas.

This is by no means a new phenomenon: Hubble (1925, *Astrophysical Journal* **62**, 409) had already described three "ring nebulae" in the spiral of the Local Group NGC 6822. But it is the advent of large narrow-band interference filters that had made possible the detection of tens of bubbles in the galaxies in our vicinity. A number of surveys have recently been published, including one by Sivan (1974, *Astronomy and Astrophysics Suppl.* **16**, 163) of our Galaxy with a 1-m telescope and one of M 33 with the Soviet 6-m telescope (Courtès *et al.*, 1981, *The Messenger* No. 23).

In our Galaxy, 21-cm surveys show numerous H I bubbles, and in fact some of the H II rings do have H I counterparts. This phenomenon is thus not restricted to ionized gas, and appears as one of the fundamental ways by which interstellar gas is being shaped in galaxies. Further kinematical and physical studies appear essential to understand the basic processes at work. Our Galaxy, however, is not quite suitable for this kind of studies: Although it has the unique advantage that one can use a home-made telescope, the observer is unfortunately embedded in the galactic disk, which reduces detection, except for close and unobscured regions. In the nearest outer galaxies (M 31, M 33, etc. . . .), the angular resolution of even the largest telescopes is not sufficient for a fair view, and detailed studies would need anyway too many of their severely distributed nights. The Magellanic Clouds—and especially the large one—appear (as usual!) as the best compromise between maximum closeness and unobstructed global view.

# N 70

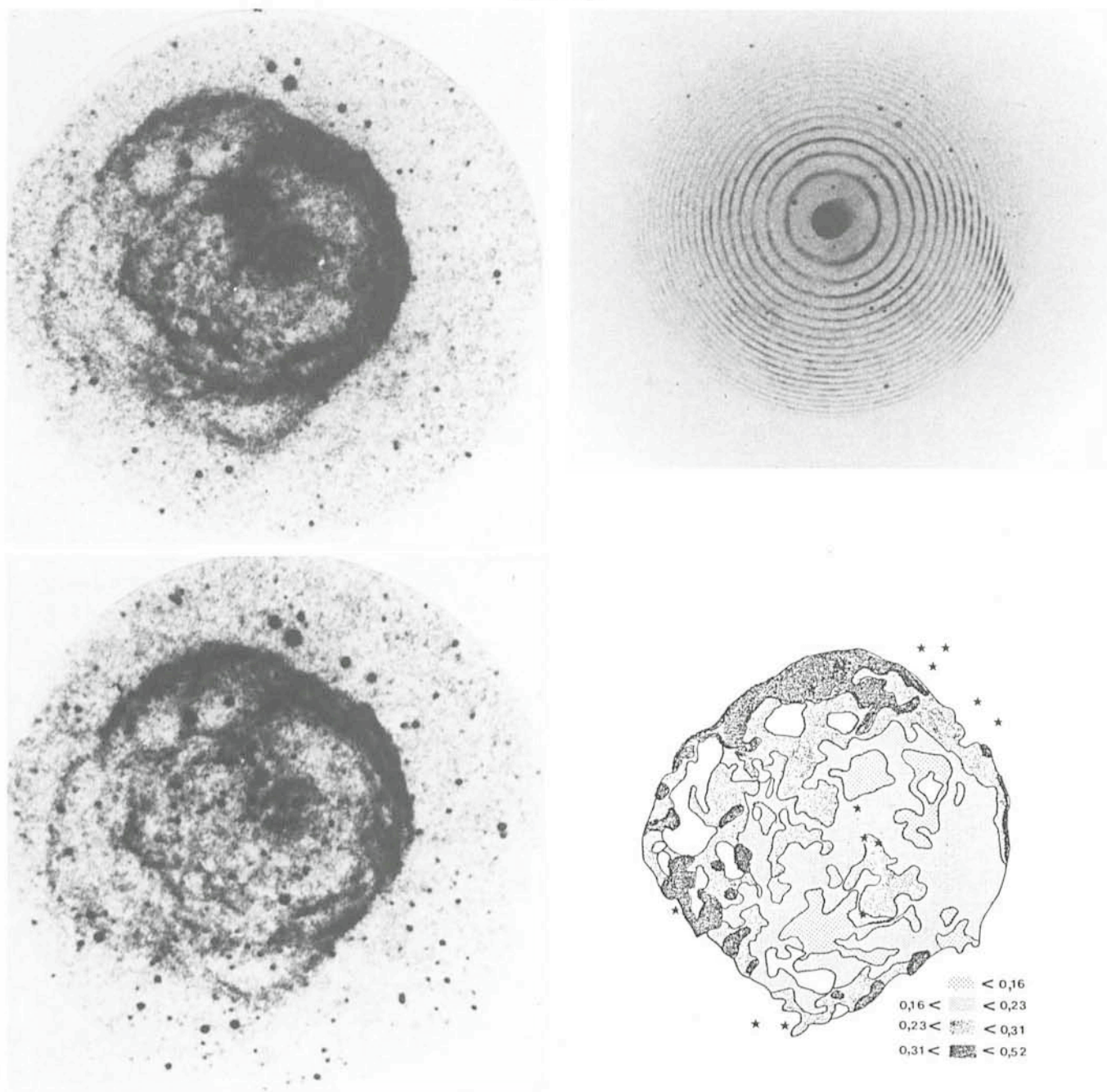


Fig. 1: N 70.

All pictures have the same orientation and scale: North at the top – Full circular field 7 arcminutes – The plates have been taken at the ESO 3.6-m telescope.

Top, left: Photograph in H $\alpha$  light. Top, right: H $\alpha$  Perot-Fabry rings projected on the nebula; Interference order  $p = 1053$  (Interfrange  $285 \text{ km s}^{-1}$ ). Bottom, left: Photograph in [S II] 6717 Å light. Bottom, right: Map of [S II] 6717 Å/H $\alpha$  ratios, using the codes given at the edge of the pictures.

## Observations

For three years we have thus carried out a quite systematic study of the bubbles of the LMC, of diameters in the range 30 to 200 pc.

The basic observational results obtained so far are:

- Radial velocity field of 20 regions with a two-dimensional Fabry-Perot Spectrograph
- Monochromatic photographs of 12 regions in the lines of H $\alpha$  6563 Å and [S II] 6717 Å.

We have observed mostly at the 1.52-m ESO telescope, plus a few occasional glimpses with the 3.6-m in the course of a kinematical programme on nearby external galaxies. Full reduction of the Fabry-Perot data is long and tedious, and till now the full velocity field has been extracted for 7 regions only. They give expansion velocities which range between a low  $15 \text{ km s}^{-1}$  (for N 23) and a respectable  $70 \text{ km s}^{-1}$  (for N 70 or N 185). A "quick-look" reduction has however been made on

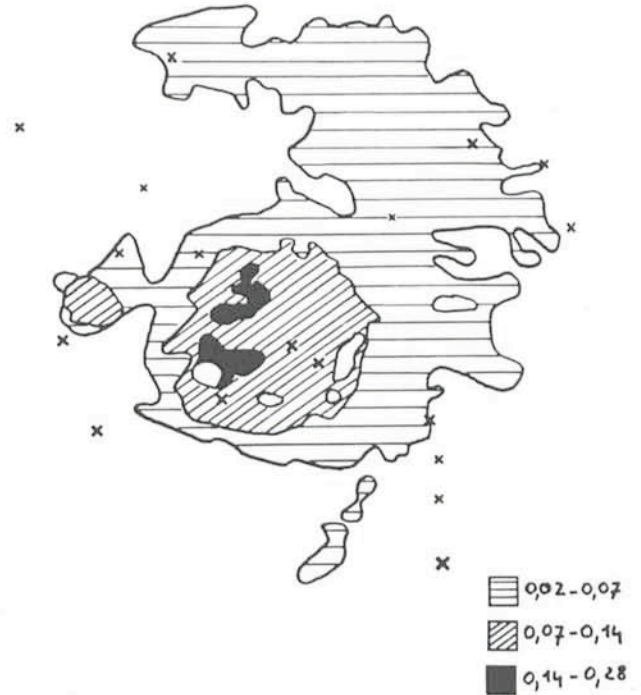
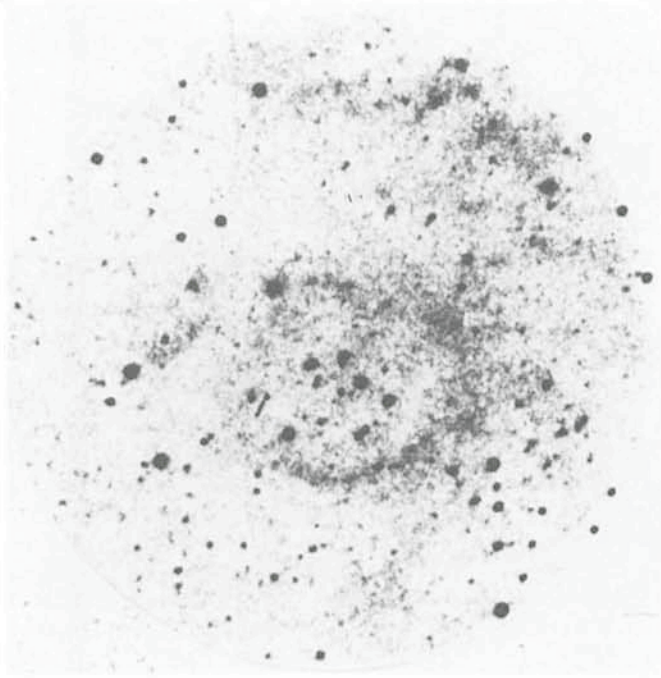
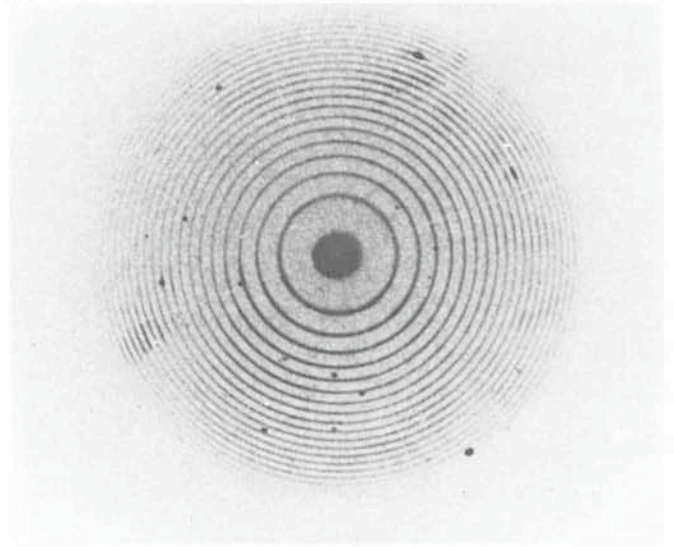
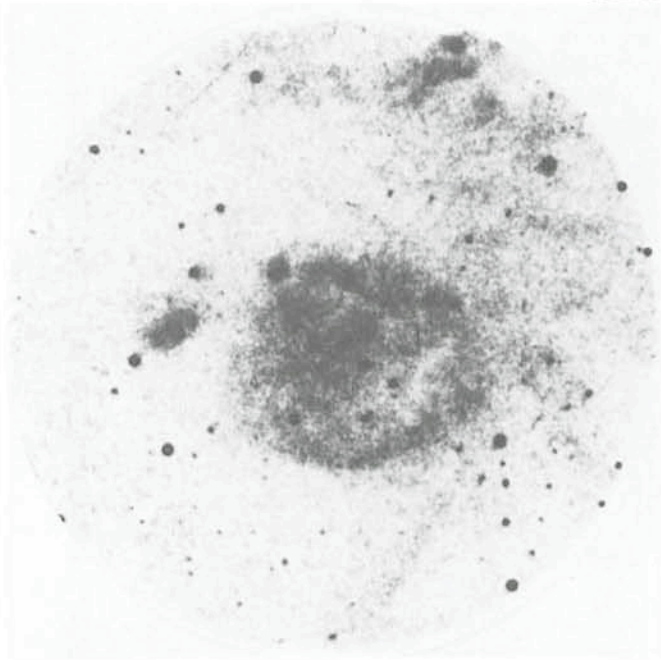


Fig. 2: N 148 I (see Fig. 1).

the 20 regions: this gives an estimation of the macroscopic turbulence and thus an idea of the strength of the shocks in the ionized gas.

Reduction of the monochromatic plates was not easy: Even with the 15 Å wide interference filter used they are all plagued with numerous stars. Lleberia (1981, IAU Colloquium, Nice), from the "Laboratoire d'Astronomie Spatiale de Marseille", has implanted a successful programme which automatically gets rid of the stars thanks to a 2-dimension topological test. We have thus been able recently to extract the [S II] 6717/H $\alpha$  ratios over the 12 nebulae studied. This ratio is also a good indicator of shocks in the interstellar medium: It is  $< 0.2$  for "normal" H II regions in the LMC and  $> 0.5$  for the well-confirmed supernova

remnants. Bubbles appear just to fill the gap with ratios between 0.2 and 0.5, indicating in general shocks of medium intensity.

Figures 1 and 2 show two extreme examples of the regions studied: N 70 (Fig. 1) is the prototype of the "strong" bubbles, with a clear crispy filamentary structure, rather large [S II]/H $\alpha$  ratios, and a large expansion velocity ( $70 \text{ km s}^{-1}$ ) superposed to chaotic motions. Its origin, however, is still much debated: old supernova remnant (Rosado *et al.* 1981, *Astron. Astrophys.* **97**, 342) or region driven by supersonic stellar winds (Dopita 1981, *Ap. J.* **246**, 65).

N 148 I (Fig. 2) is a "quiet" bubble with a less pronounced filamentary structure, faint sulfur lines, and a very small turbu-

lence ( $\sim 8 \text{ km s}^{-1}$ ). It is entirely comparable to a normal H II region. Gentle stellar winds appear as the most likely explanation.

Full correlations between the various physical quantities extracted so far will still need a few months, but the trend is already clear: Filamentary structures, large turbulence and/or large expansion velocities, and high intensity sulfur lines are usually connected, a result that can be seen as blithely encouraging or sorrowfully banal, depending on one's mood.

Some abnormal cases yet could happen: N 120—a 20 pc bubble—shows no expansion, a medium [S II]/H $\alpha$  ratio and turbulence ( $\sim 20 \text{ km s}^{-1}$  r.m.s.) and is clearly a young supernova remnant from radio data. N 48 E has the largest [S II]/H $\alpha$  ratios in our sample ( $> 1$ ) and is absent from catalogues of non-thermal radio sources.

## Conclusion

Through the detailed two-dimensional data—both kinematical and physical—obtained in the course of our study, as well as from the work of other groups, a better picture of the

processes at work is slowly emerging. There are some difficult points which, however, cast a gloom over the picture: The origin of the bubbles (SN explosions (Hodge 1967, *P.A.S.P.* **79**, 29), supersonic stellar winds (Gardis and Meaburn 1978, *Astron. Astrophys.* **68**, 189), or even collision with an extragalactic H I cloud (Tenorio Tagle 1979, ESO preprint No. 74)) is quite difficult to assess in each case. Moreover, the range of sizes goes from 20 pc diameter (N 100) to 110 pc (N 70), physical properties and diameters being not related. Some of the largest bubbles after analysis appear just heterogeneous projected structures. Especially lacking is a comprehensive survey with high angular resolution in radio wavelengths to reveal the thermal or non-thermal nature of the objects.

The edge of the bubbles, where, because of its expansion, fresh interstellar matter is being presently compressed, appears as a likely site for generation of new stars and could—according to the so-called “contagion hypothesis”—explain the large-scale chaotic appearance of spiral arms in galaxies. Star formation however appears too erratic in the Magellanic Clouds, and we must turn to more distant, but more regular spirals.

# Large-Scale Structure of the Universe

Guido Chincarini, University of Oklahoma

One of the major tasks of astronomy is to find how matter is arranged and distributed in our Universe. On the largest scale it has usually been assumed by cosmologists and by the majority of astronomers that matter is spread uniformly throughout the Universe. This picture is changing and astronomers are recognizing, by focussing more and more on the study of the distribution of visible matter, that the distribution of galaxies is very clumpy on a small scale (pairs and groups) as well as on a much larger scale (superclusters or filamentary structures). It is not clear, in fact, whether any isolated structure exists.

We can preserve homogeneity, but only on a much larger scale than was previously recognized. An observer located in a different part of the Universe could not distinguish one location from the other over scales larger than 50–100 Mpc. The main characteristics would remain the same. For an excellent review and discussion on this matter see Chapter 1 of “The Large-Scale Structure of the Universe”, by Peebles (1980).

Evidence that the surface distribution of matter is clumpy has been collected, even if somewhat disregarded until recently, since long ago. I refer to the catalogue by Messier of 1784, to the surveys by the Herschels in the 18th and 19th centuries, to the work by Shapley and Ames (1932, *Harvard Obs. Ann.* **88**, No. 2) and to the later work by Shapley on the distribution of galaxies. Four more recent surveys are of particular importance: The survey of clusters of galaxies by Abell (1958, *Astrophys. J. Suppl.* **3**, 211), the catalogue of galaxies and clusters of galaxies by Zwicky and coll. (1967), the counts of galaxies by Shane and Wirtanen (1967, *Pub. Lick Obs.* **22**, part 1) and the counts in the Jagellonian field by Rudnicki *et al.* (1973, *Acta Cosmologica* **1**, 7). The distribution of galaxies is clumpy also in depth. The first evidence came during the observations of a non-cluster field near the Seyfert sextet located north of the Hercules cluster A 2151 (Chincarini and Martins, 1975, *Astrophys. J.* **196**, 335). However, this evidence was based on a sample of ten galaxies only. The first confirma-

tion of this result was obtained by Tifft and Gregory (1976, *Astrophys. J.* **205**, 696) from the study of a larger sample.

During the seventies two lines of studies developed independently. On the one hand, various astronomers intensified studies on the detailed three-dimensional distribution of galaxies in large regions of the sky; on the other hand, thanks especially to Peebles (1974, *Astrophys. J. Letters* **189**, L51), a sophisticated autocorrelation analysis was developed and extensively applied to the interpretation of counts of galaxies<sup>1</sup>. Previously Totsuji and Kihara (1969, *Publ. Astron. Soc. Japan* **21**, 221) had derived, using an autocorrelation analysis and the catalogue by Shane and Wirtanen, the same coefficients for the autocorrelation function:  $g(r) = (r_0/r)^{1.8}$  with a characteristic length  $r_0 = 4.7$  Mpc. Their work went unnoticed for some time.

Ideally we should have a catalogue, or a random subsample of it, complete to a reasonably faint magnitude giving redshifts (possibly accurate to better than 50 km/sec), magnitudes, morphological types and positions. Such a work has been undertaken by Davis from the Center for Astrophysics in Cambridge, Mass.

It appears, today, that galaxies are not distributed at random and that clusters of galaxies are not isolated systems. The distribution of pairs of various separation is described by the autocorrelation function. The function is a measure of the deviation from a random distribution. It also measures the characteristic size of clumpiness and allows confrontation of theories on the clustering of galaxies with observations. Studies on selected regions of the sky show the existence of very asymmetric, often filamentary-like structures, separated by regions which are void of galaxies.

Oort, Arp and de Ruiter (1981, *Astron. Astrophys.* **95**, 7) give evidence that quasars are part of superclusters and Burns and

<sup>1</sup> Peebles' understanding of the cosmological significance of the analysis of the data became a guide to theoretical and observational work and to its physical interpretation.

Owen (1979, *Astron. J.* **84**, 1478) show that such large structures can also be recognized from the distribution of radio sources. (In Figure 1 is a reproduction of the largest one recognized so far and connecting the Hercules complex to the group of clusters A2197–A2199.)

Our Galaxy is part of such a structure: the Local Supercluster. The Local Supercluster was recognized by the work of Shapley and Ames (1932), extensively studied by de Vaucouleurs (1956, *Vistas in Astronomy* **2**, 1584) and most recently by Yahil, Sandage and Tammann (1980, *Astrophys. J.* **242**, 448), after completion of the observations of the galaxies of the Shapley-Ames catalogue. This structure may be tenuously connected to others, it is dominated by the Virgo cluster of galaxies towards which we may be falling (Aaranson *et al.* 1979, *Astrophys. J.* **239**, 12).

Following the IAU symposium in Tallin (1978), theoretical and observational works are flourishing and our understanding deepening and progressing very fast. It is exciting because it makes us sense the satisfaction of mapping an as yet unknown world, but what are the goals? Knowledge on how the distribution of visible matter is structured at the present cosmological time will essentially ask for theories which are able to explain how and when such structures and voids (density fluctuations) were formed in an expanding Universe. Observations have therefore to define clearly the basic parameters of the distribution of visible matter. The irregular distribution of matter, furthermore, causes gravitational pulls at large distances so that by studying the statistical distribution of gravitational forces and masses we may be able to detect and understand peculiar motions of galaxies and measure the mean mass density of the Universe. We already have estimates of this parameter, the problem is that in this case, and at this phase of the game, we have too many determinations so that almost any value between 0.01 and 1 has been derived. Certainly the understanding of the large-scale structure will also give insights in the processes of galaxy and cluster formation.

In 1977, after we read the work of Shapley, "A catalogue of 7,889 external galaxies in Horologium and surrounding regions", M. Tarenghi and myself became interested in the study of this region of the southern sky. Together with P. Crane, J. Materne and Hélène Sol we are now working on it.

The Horologium region appears to be extremely complex. As pointed out by Peebles, some of the irregularities in the distribution are certainly introduced by vignetting at the edge of the photographic field, the majority of the structures are, however, real. Groups and clusters are packed together and embedded, probably, in a supercluster dispersed component expanding with the Hubble flow. Cluster-cluster interaction and cluster accretion may be at work so that it may become a serious problem to disentangle, and correctly interpret, the redshifts. On the other hand such complicated regions are rich in information and need also to be accounted for from theoretical models.

We selected from Shapley's catalogue a random sample of about 300 galaxies for which we obtained redshifts using the observing facilities of La Silla (ESO) and Cerro Tololo (I.A.O.). In addition we observed all the galaxies brighter than  $m = 15.0$  and Manousoyannaki and H. Sol obtained at La Silla (ESO) B and V photoelectric magnitudes for more than 100 galaxies. The majority of redshifts are in the range between 7,000 km/sec and 22,000 km/sec with groupings at about 8,000 km/sec, 11,000 km/sec and 17,000 km/sec. The cluster CA 0340–538, part of one of the observed superclusters, is at a distance of 17,400 km/sec; it is also an extended source of X-ray emission.

From the observations of simpler structures, Perseus-Pisces and Coma-A1367 (these seem to look like filaments almost perpendicular to the line of sight) it is possible to estimate that

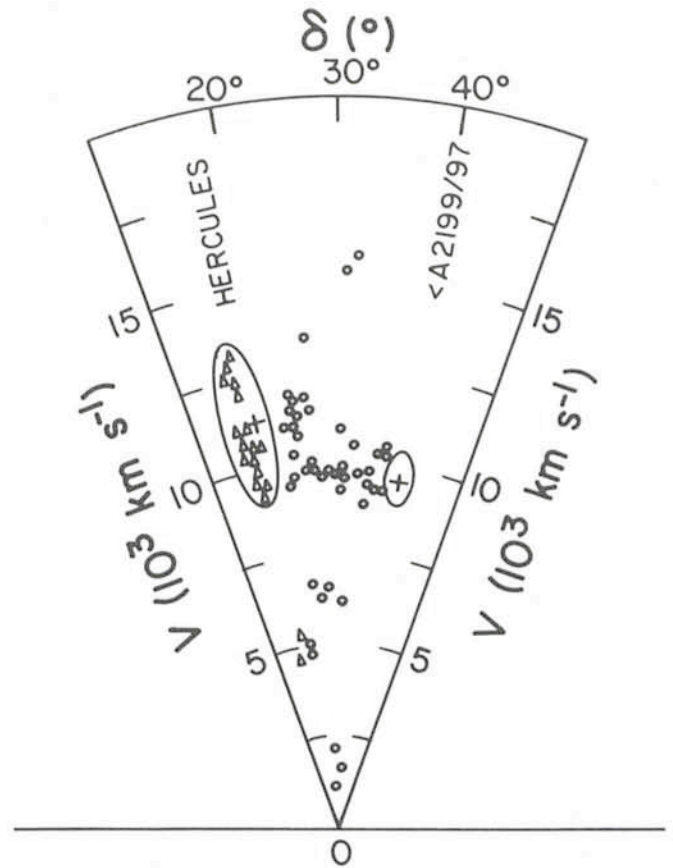


Fig. 1: Redshift vs. declination for a subsample of galaxies between the two clusters A 2197/99 and A 2151. The two groups of Abell clusters are represented by large oval outlines (From *Astrophys. J. Letters*.)

these superclusters are about 500 km/sec in depth, 50–100 Mpc in the other dimension (since these structures may be interconnected such estimates may be of limited significance), have a column density of about  $10^{-4}$  gr/cm<sup>2</sup> and a mass (for the part of the supercluster which has been observed) of about  $10^{16}$  solar masses. The dispersed component is not very massive and its mass is of the order of magnitude of the mass of a cluster of galaxies (Chincarini 1981, preprint). By interpreting the Ly $\alpha$  absorption in quasars as originating in a supercluster gaseous component left over during the process of galaxy formation, Oort (1981, *Astron. Astrophys.* **94**, 359) estimates a gas column density of about  $6.8 \cdot 10^{-4}$  gr/cm<sup>2</sup>.

Further information will be added from the 21-cm survey that Giovanelli, Haynes and the author have been carrying out at the Arecibo Observatory since 1977.

These data will make possible the determination of the hydrogen and total masses of the supercluster galaxies. It is possible, therefore, not only to measure the hydrogen deficiency as a function of the location of galaxies in a supercluster (Giovanelli, Chincarini, Haynes, 1981, *Astrophys. J.* in press), but to determine the distribution of galaxy masses in the supercluster and whether the masses of the single galaxies are correlated with the density of the supercluster. We are progressing very fast towards the understanding of the distribution of visible matter in the Universe; even faster progressing are the theory and the understanding of the evolution of these structures thanks to the work of Peebles, Gott, Zeldovich, Doroskhevic, Novikov and many others. All these new developments, data and interests are bound to generate in the coming years a deeper enlightening understanding.

# The Discovery of a New SU UMa Star

Bernd Stolz, *Universitäts-Sternwarte München*

For the observing run in November/December 1980 at La Silla, R. Schoembs and myself had a strict observing schedule long before travelling to Chile in order to make best use of the allotted instruments. A usual behaviour common to all astronomers, I think. But a lucky chance made us change our plans in some details on the spot: We discovered a new member of the SU UMa subgroup of dwarf novae.

It's my aim to tell some of the exciting circumstances of that discovery and to report some results of the measurements of the new SU UMa object TU Men.

## Dwarf Novae, a Subgroup of Cataclysmic Variables

Dwarf novae belong to one of the four subgroups of the cataclysmic variables. The denotation *cataclysmic* originates from the ancient Greek word *κατακλυσιμός* which means catastrophe or deluge. This describes the main property of these objects to erupt with more or less catastrophic consequences for the whole system. According to a generally accepted model a cataclysmic variable consists of a very close binary system. The primary component is a white dwarf surrounded by a disk of matter of low density. The companion is very similar to a red main-sequence star. Both circulate on their orbits with rather short periods, mostly within the range of 1–10 hours with an empty gap between 2–3 hours. This remarkable period gap is of great importance from the point of view of stellar evolution (see H. Ritter, 1980, *The Messenger* No. 21, p. 16). There is a mass flow from the red secondary towards the white dwarf. Where that stream impacts the accretion disk the material heats up and a bright hot spot is produced. (Figure 2 in the article of H. Ritter presents a beautiful picture of the model of a cataclysmic variable.)

Caused by some unknown mechanism dwarf novae suddenly erupt from time to time. Then the brightness of the system increases within hours by a factor of 100 and the spectrum mainly changes from an emission-line to an absorption-line spectrum. Such an outburst lasts about a few days and repeats in the order of weeks.

This short and rough presentation of the scenario of a dwarf nova system cannot compensate for an exact description of the theoretical model and all of its characteristics. More details are given for example in the review article of E. L. Robinson (1976, *Annual Review of Astronomy and Astrophysics*, Vol. 14, p. 119) or B. Warner (1976, *IAU Symp.* No. 73, p. 85).

## SU UMa Stars, a Subgroup of Dwarf Novae

The research on cataclysmic variables has got new aspects during the last years due to the discovery of the so-called SU UMa stars. These objects have additional striking properties compared with normal dwarf novae. For example, a second kind of outbursts occurs. These eruptions are called super-outbursts because they last much longer than the normal ones and the maximal brightness exceeds that of a short outburst. The recurrence time is of the order of months and so much longer than that of normal maxima. The most puzzling property, however, is the superhump-phenomenon. In the course of a super-outburst a periodic feature in the light-curve—the superhump—appears, which does not repeat with the orbital period measured spectroscopically for example. The superhump period  $P_s$  is always longer than the orbital one by a

few per cent. The understanding of that phenomenon, observed for SU UMa stars during super-outbursts only, is not satisfactory as yet. One of the most recent models explaining the observational facts of SU UMa objects is presented by N. Vogt (1981, ESO preprint No. 138) who assumes an eccentric disk around the white dwarf formed during a supermaximum. For more details dealing with models and observational facts I have to refer to this work or to a review article of N. Vogt (1981, *Astronomy and Astrophysics*, Vol. 88, p. 66).

## TU Men, a Possible SU UMa Candidate

For the observing run in November/December 1980 on La Silla, checks for outbursts of more or less unknown dwarf novae had been planned as a supplement of the main programme. During the preparation at home, I had paid special attention to possible SU UMa candidates. One of those objects was TU Men, a faint dwarf nova (brightness  $m_v \geq 16^m$ ). During 1963 and 1978 TU Men had been observed in many nights by several members of the variable star section of New Zealand. On these observations F. M. Bateson (1979, *Publ. Var. Star Sect., Roy. Astron. Soc. New Zealand* 7, p. 5) based his assumption that two groups of outbursts could be distinguished: Faint eruptions ( $m = 13^m$  5), which last approximately 1 day and recur every 37<sup>d</sup>, and bright eruptions ( $m = 12^m$  5), which last 4–20 days recurring every 194 days. TU Men therefore seemed to possess two characteristics of SU UMa stars and had been included in the observing programme.

At the end of the first observing night on La Silla we had a look at TU Men and found the star in a state of outburst. Because of that new situation we rearranged the time schedule and decided to observe TU Men photometrically in the second night from the beginning.

## TU Men, a New SU UMa Object

To our great surprise the brightness of TU Men seemed to increase immediately after starting the measurement. Checking the electronic equipment and the intensity of the comparison star we convinced ourselves that this variation was real. A few minutes later the brightness decreased again to reach a constant level. In that moment we suspected for the first time a super-outburst for TU Men and the evidence of a superhump phenomenon. To confirm that, we had to measure several superhumps and we expected the next one at the latest about 2 hours after the first one. This assumption was based on the fact that all SU UMa stars already known belonged to the ultra-short-period cataclysmic binaries with periods below the well-known gap between 2 and 3 hours. But the chart recorder continued to display constant brightness even 2 hours after the first one! Thirty minutes later we were almost completely disappointed when finally the rise to the second superhump took place! At the end of that night we had recorded 3 superhumps of TU Men recurring with a period of about 3 hours! Following the rule that the orbital period  $P_o$  and  $P_s$  differ by a few per cent only, the long superhump period of TU Men indicated that SU UMa objects could be found even beyond the period gap. To verify this assumption, besides an accurate photometry of TU Men it was important to determine the orbital period by means of spectroscopic observations. So TU Men had changed from a substitute to the main object in one night.

## Photometric Observations of TU Men

The lightcurve recorded during a time interval of 16 days is shown in Figure 1. The measurements have been obtained with the 50-cm Danish, the 62-cm Bochum, the 1-m ESO and the 1.5-m Danish telescopes. The lightcurve shows the periodic superhump phenomenon. The amplitude of the variations decreases from  $\Delta m = 0^m.36$  during the first two nights to  $\Delta m = 0^m.13$  at the end of the observations.

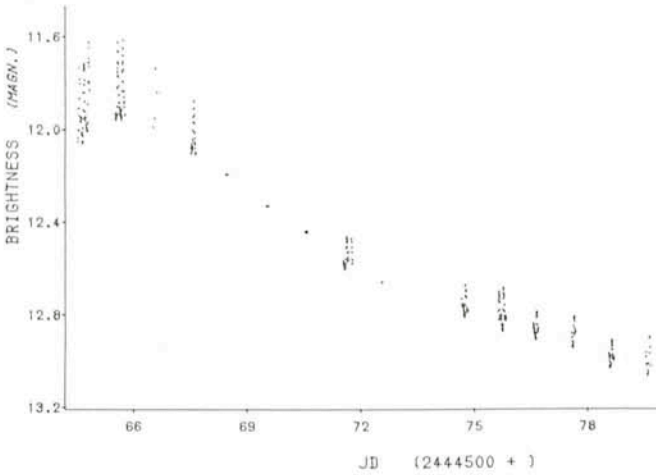


Fig. 1: Lightcurve of TU Men over the whole observing run (1980, Nov. 20 – Dec. 6).

The superhump timings cannot be described by a constant period. With a period  $P$  determined from the first two nights, one gets a phase shift reaching  $1.4P$  for the last recorded superhump. So, as in the case of other SU UMa stars, a linearly decreasing period has been adopted for the superhumps. A least-square fit to the observed timings of maximal brightness yields the following ephemerides:

$$\text{HJD} = 2444564.584 + .1262 E - 6 \times 10^{-6} E^2.$$

## Spectroscopy of TU Men

The spectroscopy of TU Men has been performed in 4 nights at the 1.5-m ESO telescope equipped with the IDS.

All 42 spectra show the typical very broad Balmer absorption lines of dwarf novae during outburst. A sine curve has been fitted to the mean velocities of each spectrum. The minimum of rms-error is obtained for the period

$$P_0 = 2.820 \text{ hours} = 0^d.1176 \pm 0^d.0007$$

Figure 2 shows the resulting phase diagram. The result indeed confirms the assumption that SU UMa stars are not restricted to the ultra-short-period cataclysmic binaries below the period gap.

## The $P_s \leftrightarrow P_0$ Relation

Including TU Men and WZ Sge, orbital and superhump periods are known for 7 objects. (Because normal outbursts fail to appear, WZ Sge is not a SU UMa star in the common sense. Nevertheless, a superhump phenomenon has been detected for that system. See J. Patterson et al., 1981 *Astrophys. J.* Vol. 248, p. 1067.) With these data a relation between  $P_0$  and  $P_s$  can be established. This has been done in Figure 3, which shows  $(P_s - P_0)/P_0$  versus  $P_s$ . The points are well fitted by a parabola; this is probably due to the small number of points

used; however, if this relation is supposed to be correct, it allows to compute the orbital periods for SU UMa objects of known  $P_s$ .

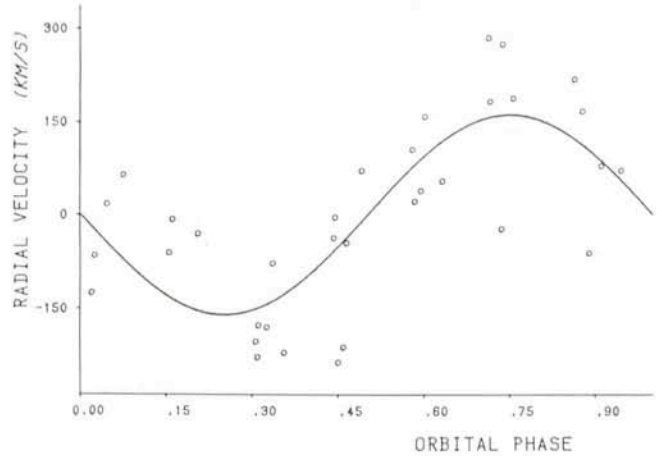


Fig. 2: Radial velocity curve of TU Men obtained during the super-outburst in December 1980.

One consequence of the observations of TU Men and the derived relation between  $P_s$  and  $P_0$  is that the period gap of CV's shrinks to forty minutes: On one side there is the observed orbital period  $P_0 \approx 2^h50^m$  of TU Men, on the other side the computed period  $P_0 \approx 2^h10^m$  of YZ Cnc.

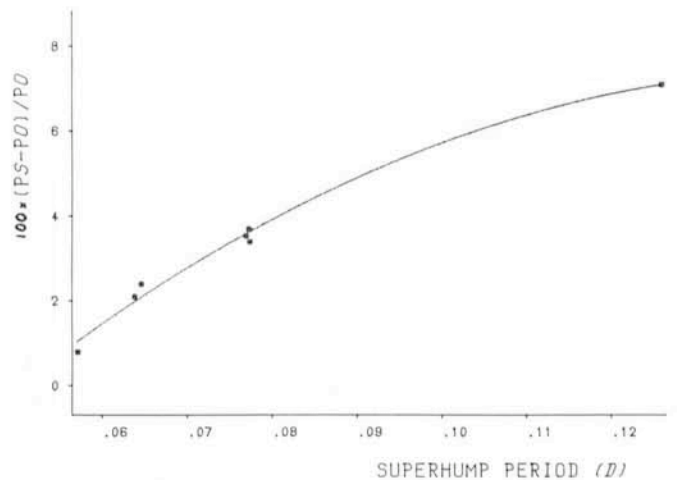


Fig. 3:  $(P_s - P_0)/P_0$  versus  $P_0$  for seven objects with known orbital and superhump period.

I hope that this report has given an impression of our work on dwarf novae, especially on SU UMa stars and an idea of our exciting experiences during the night when TU Men was discovered to be a member of that subgroup of CV's. For me it was the first time on La Silla and I never believed in having such good luck to receive so many data from such an interesting object.

Last not least we want to express our thanks to all staff members and night assistants, especially Dr. H. Pedersen and J. Veliz.

# The Uranus Occultation of August 15, 1980

Patrice Bouchet and Christian Perrier, ESO

André Brahic, Jean Lecacheux and Bruno Sicardy, Observatoire de Paris

## The Rings of Uranus

One of the very exciting discoveries in astronomy and planetary sciences in recent times is the detection of a series of narrow rings around Uranus. During more than three centuries, the rings of Saturn have had a special fascination and symbolism and an enormous amount of literature has been devoted to studies of their nature, properties and origin. The discovery of Uranus' rings, and two years later of Jupiter's rings has not only renewed interest but also raised a number of new cosmological questions.

Planetary rings are important not only because of the dynamical problems which they pose, but also because it is probable that processes which played a role in planet and satellite formation are still at work in these rings: ring systems afford a good opportunity for studying some of the accretion mechanisms which operated in the early solar system. Techniques used for galactic dynamics have been particularly fruitful for the understanding of planetary rings. Conversely, a detailed study of ring structure can lead to a better understanding of other flat systems like spiral galaxies or accretion disks. Collisions which play such an important role in the Universe can be studied in rings. Furthermore, particles of planetary rings are natural probes of the internal structure of the central planet.

## Discovery of the Rings of Uranus

It is almost impossible to observe directly from the Earth a system of dark rings of 8 arcseconds around a planet which has an apparent diameter of 4 arcseconds. The Uranian rings have been discovered during the occultation by Uranus of the late-type star SAO 158687 of visual magnitude 9.5 on March 10, 1977. High-speed photometry of occultations provides a powerful tool for probing the upper atmosphere of a planet, as has been shown during the past decade from occultations involving Mars, Jupiter, and Neptune. In 1977, all of these efforts paid off when not only the predicted occultation by the planet, but also a series of secondary occultations by the previously unsuspected rings, were observed (Elliot *et al.*, 1977 a, b; Millis *et al.*, 1977). It is pleasant to note that occultation techniques are very powerful: they give a resolution slightly better than the one obtained from a Voyager-type spacecraft flying by the planet. From the Earth, the resolution is limited by Fresnel diffraction and by the angular size of the occulted star.

## Deductions from Observations

Seven useful occultations have been observed up to now. The Uranian rings pose a number of new and unexpected dynamical problems. At least nine rings encircle the planet, extending between 1.60 and 1.95 planetary radii. Compared to their circumference (some 250,000 km), they are exceedingly narrow: most do not exceed 10 km in width and only one, the outermost ring, spans as much as 100 km. Three rings are circular, but six are eccentric and have variable widths. Both of these characteristics are best illustrated by the external ring: it is the largest, its distance from Uranus varies by about 800 km and its width changes from 20 to 100 km linearly with its distance from Uranus. The remarkable thing is that these

elliptic rings precess slowly about the planet ( $1.364^\circ$  per day for the outer ring). Normally, the rate of precession around an oblate planet would depend on the distance to the planet and this differential precession would shear each ring into a circular band. In fact, each ring precesses as a rigid body. The profile of the rings looks the same everywhere. The rings have sharp outer edges, and structure bigger than noise appears within a number of rings. A more detailed review of the observations is given by Elliot (1981) and Brahic (1981).

## Ring Dynamics

Similar intriguing situations have been recently observed around Saturn and Uranus by Voyager spacecraft (narrow rings, eccentric rings, sharp edges, nearby satellites, . . .). It seems that a confining mechanism which played a role for the formation of planets and satellites is actually at work in ring systems.

Unconfined rings of free colliding particles spread under the combined effect of differential rotation, inelastic collisions, and Poynting-Robertson drag (Brahic, 1977; Goldreich and Tremaine, 1978). Resonances with known satellites are too weak and too few to explain the observed features directly.

A satellite near a ring of colliding particles exerts a torque on the ring material. They exchange angular momentum; this leads to a mutual repulsion of the ring and the satellite. Like in a spiral galaxy, a nearby satellite creates leading and trailing spiral density waves which are controlled by a combination of the Coriolis force and the ring's own gravity. Small undetected satellites on each side of the ring could constrain its edges and prevent ring spreading; elliptical rings can also be generated by such a confining mechanism. Kilometre-sized bodies are massive enough to confine the observed rings. They are the largest "particles" of the original ring (Goldreich and Tremaine, 1980; Hénon, 1981).

## The Occultation of August 15, 1980

Time was allocated at the 3.6-m telescope for the occultation of the star KMU 12 (Klemola and Marsden, 1977) by Uranus and its rings.

It was the first Uranus occultation successfully observed by a European team. The best signal-to-noise ratio was observed during this occultation. New features were discovered in the ring system and new information obtained on the atmosphere of Uranus. Two American teams around Elliot, Nicholson and Goldreich, working with the large telescopes at Las Campanas and Cerro Tololo observatories obtained data of similar quality. It was the first time that an occultation had been observed, with such quality of results, from three different points simultaneously. The reduction of the data is being done in the frame of a common American-European programme and is leading to new results. The ESO data are being reduced by Bruno Sicardy. The study of correlations is particularly important.

## Observations

The observations were made using the new infrared photometer mounted on the 3.6-m telescope at La Silla. A standard K

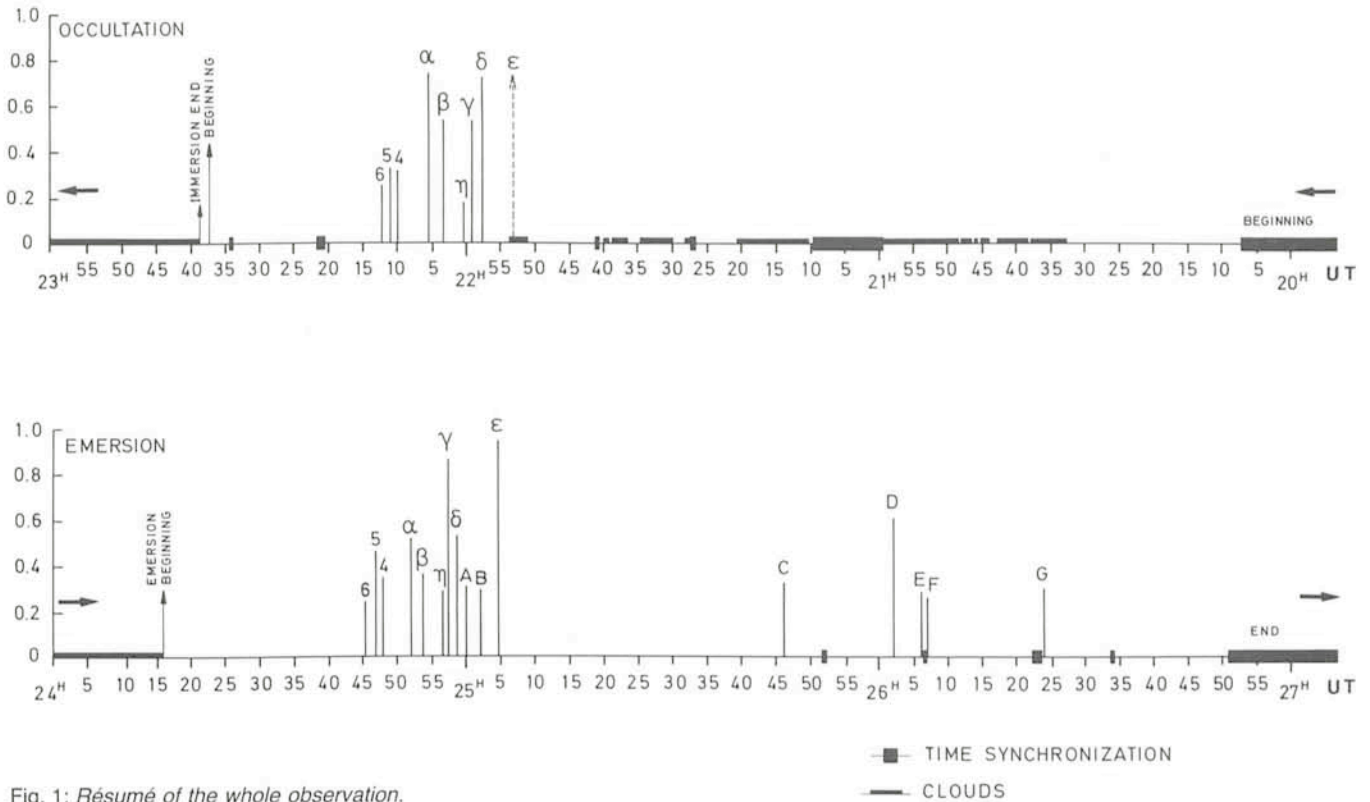


Fig. 1: *Résumé of the whole observation.*

filter ( $\lambda_0 = 2.20 \mu\text{m}$ ;  $\Delta\lambda = 0.5 \mu\text{m}$ ) was used with an InSb detector cooled to  $55^\circ\text{K}$ . The choice of this wavelength is due to the strong methane band which greatly depresses the light reflected from the planet. Actually, at this wavelength, the albedo of Uranus is only  $10^{-4}$ . Thus, quite fortunately, the star KMU 12 ( $K = 8.5$ ) was considerably brighter than the Uranus system at  $2.2 \mu\text{m}$ , giving a high contrast during the eclipses. Sky subtraction was achieved by chopping at 18 Hz to a secondary beam located  $20''$  to the South. An aperture diameter of  $10''$  was selected to reduce thermal background noise without introducing noise from guiding and seeing effects. Therefore, the noise was mainly due to detector and background radiation from the telescope and the sky. A signal-to-noise ratio of  $\sim 100$  could be achieved with a time resolution of 0.1 s.

Thanks to F. Gutiérrez, at La Silla, who promptly wrote for these observations a new version of the fast acquisition programme, it was possible to record the signal with a "sampling period" of 0.1 s. UT was drawn directly from the La Silla caesium clock and automatically controlled every 10 s, and reset if necessary. This was rather risky since this resetting could have occurred precisely during a ring occultation, but fortunately that did not happen.

The star was centered by finding the half-power points of the  $2.2\text{-}\mu\text{m}$  signal 45 minutes before the first occultation and centering was maintained during daytime trying to keep the signal to this level. The excellent tracking of the telescope and the tests performed the previous night to find the optimum tracking rate, plus the fact that we were looking at rapid decrease of the signal, rather than slow variation, allowed us to proceed in such a way. As soon as it became possible—right after emersion from Uranus—we used an offset-guider/Quantex TV-system to maintain centering. During the occultation by the planet itself it was impossible to point dead on the star, which explains our lack of accuracy at emersion.

Uranus' centre passed  $0.7 \pm 0.3$  S-SW of the star. As the planet's apparent radius was  $1.9''$ , its disk completely occulted

the star. The span of the ring system being  $7''$ , it was almost diametrically crossed by the path of the star. Note that all crossing times occurred 10 minutes earlier than predicted. The first one (star passing behind ring  $\epsilon$ ) was observed through clouds at around 21 : 50 UT. Luckily, clouds vanished completely right after, which allowed us to see the rings passing in front of the star during the following half hour.

Sunset occurred at 22 : 30 UT. At 22 : 31 UT the star disappeared progressively during 3 minutes. The record then shows many randomly scattered and very fast jumps or spikes in the signal. The progressive shape of the lightcurve is due to refraction in Uranus' atmosphere (exponentially decreasing distribution of its density with altitude) while scintillation in it caused the spikes. After  $\sim 1 \frac{1}{2}$  hour of total eclipse, the star reappeared exactly as it had disappeared, its path crossing the ring system in reversed direction.

### Preliminary Results

Figure 1 shows the depth of the observed events vs. UT. Rings  $\alpha$ ,  $\beta$ ,  $\gamma$ ,  $\delta$ ,  $\eta$ ,  $\epsilon$ , 4, 5 and 6 are the already known ones, as they were first identified. Events A, B, C, D, E, F and G are

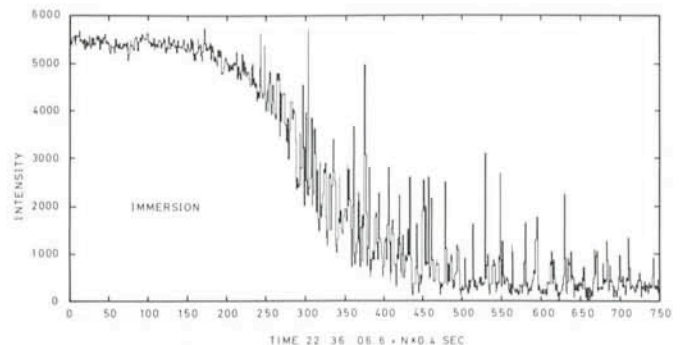


Fig. 2: *Immersion of the star behind the planet.*

possible new phenomena which we may have observed and which will be discussed later.

Figure 2 shows the immersion of the star behind the planet. This interesting lightcurve may unveil some fundamental aspects of Uranus' atmosphere and mesospheric temperature.

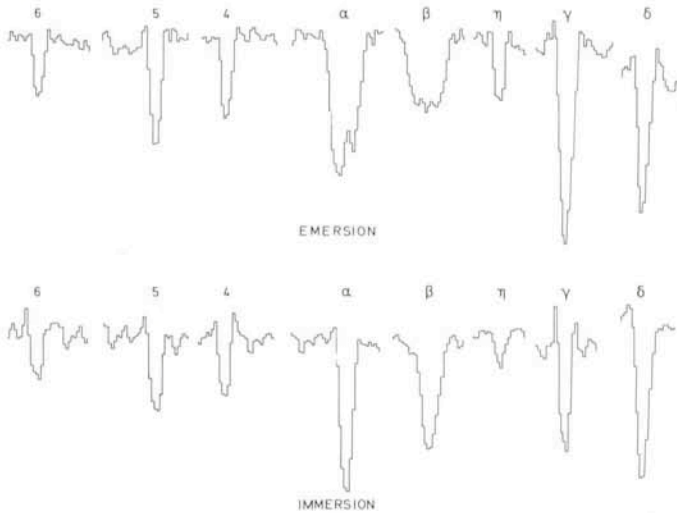


Fig. 3: Observed occultation profiles of rings  $\alpha-\eta$ .

Figure 3 depicts the observed occultation profiles of rings  $\alpha-\eta$  and Figure 4 that of ring  $\epsilon$ , unquestionably the most intriguing. The similarity of these profiles with already observed ones (Nicholson *et al.*, 1978; and for the same event, Elliott *et al.*, 1980) is evident. Note, for instance, the "double-dip" structure of the  $\alpha$  ring and diffraction fringes mainly at the edges of the  $\gamma$  ring, but present in other rings as well.

Another important result is the lack of evidence, at the 5% level, of any smoothly varying background absorption. This feature is also in agreement with Nicholson *et al.* (1978) and Elliot *et al.* (1977 a, b, 1980).

A new and most exciting aspect of our observations is that we may have observed further significant occultations. Figure 5 samples profiles corresponding to the more prominent of these events. Striking as it may seem, observers at Cerro Tololo and Las Campanas recorded no occultation at these particular times. Nevertheless, we do feel that these phenomena are real—although a possible instrumental or atmospheric origin cannot be totally excluded—for the following reasons:

(a) Although cirri were present at the very beginning of the observations, it seems that they disappeared later and did not disturb the observations from the occultation of ring  $\delta$  on.

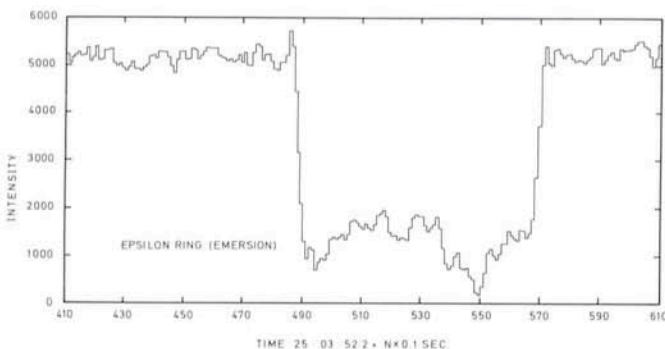


Fig. 4: Observed occultation profile of  $\epsilon$ -ring in emersion.



Fig. 5: Observed profiles of possible events (see text).

Anyway, the time scales of the variations due to the presence of cirri are far longer than those of the actual occultations. Moreover, they never look like isolated spikes, as is the case in our reported events.

(b) Also questionable is the argument that attaches their origin to bad centering. Indeed, these new occultations were detected during night-time with an offset-guider/Quantex-TV system allowing excellent *guiding* and we noticed no decentering at all. Furthermore, immediately after each reported event we recorded the same stellar flux and noise levels as just before them. This would have been very difficult to achieve had there been a decentering effect using a system which did not give in that time, an optimum beam profile.

However, apart from the explanations mentioned above, we feel another situation is worth reporting. Once the observations of the actual occultations were over, we kept on centering on a star with the same K magnitude. This was done during one hour in order to check for any variations in the signal. Here we were *lucky* enough, though rather disappointed, to observe an effect which may be called "seeing fluctuation". The result is the same profile as observed for some known rings as well as possible new events.

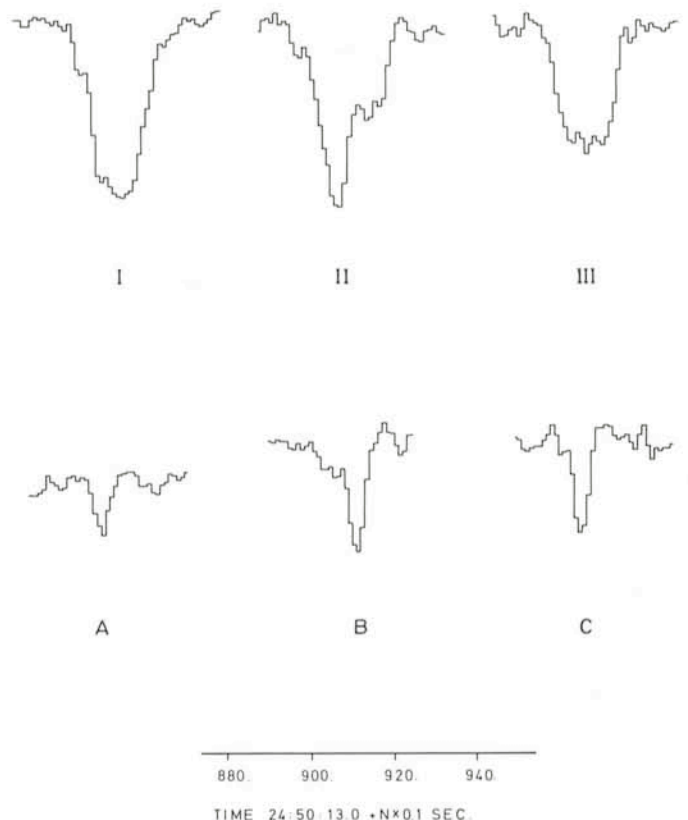


Fig. 6: "Play with us" (see text).

So the question is open! Are these observations reflecting real events? (IAU Circ. No. 3503 and No. 3515.) Maybe the answer lies in the results of future observations. Meanwhile, let us consider Figure 6 which gives an idea of the problem.

With the same stellar flux level, I, II and III in this figure show the profile obtained with an intentional decentering (followed by immediate recentering, what we never did during the observations), the one of a possible newly discovered event, and the one of a known ring, respectively.

In the same figure, A, B and C correspond to the profile of a known ring, a seeing fluctuation and a possible event. Which is which?

Finally, let us recall the events reported by Churms (1977) and Millis and Wasserman (1978) during the March and December 1977 occultations and which have never been confirmed. On the other hand, one should bear in mind the fact that Nicholson *et al.* (1978) claimed that rings 5 and 6 are not two complete rings, but rather a collection of incomplete arcs. Again, only future occultations, preferably observed with telescopes less than 1 km apart, will throw more light upon the question of whether these random phenomena are caused, as suggested by J. Lecacheux (1980) by a profusion of large boulders not organized to form a ring.

## Conclusion

The result of this observation will be published in the next months. Here, we can only give an abstract of the main results:

– The already observed structure of the rings has been confirmed and additional features have been discovered such as broad structures near the narrow rings. Rings have a very complex internal structure and the existence of incomplete arcs or additional satellites around Uranus has to be investigated.

– The observations from La Silla, Las Campanas and Cerro Tololo are used to compare the structure of the atmosphere of Uranus at points separated by about 100 km, along the plane-

tary limb. There are striking, but not perfect, correlations of the lightcurves. This rules out the isotropic turbulence as the cause of lightcurve spikes. The atmosphere is strongly layered and its mean temperature is  $150 \pm 15^\circ\text{K}$ .

In order to have a better understanding of the dynamics and the structure of the rings and the atmosphere of Uranus, it is necessary to observe additional occultations, each one being a high-precision scan of the planet and its rings, in order to reconstitute point by point the ring system.

## References

- Bouchet, P., Perrier, Ch., Sicardy, B. IAU Circulars, No. 3503 and No. 3515.
- Brahic, A. (1977) *Astron. Astrophys.*, **54**, 895.
- Brahic, A. (1981) in Uranus and the outer planets (IAU/RAS Colloquium No. 60, G. Hunt ed.), Cambridge University Press.
- Churms, J. (1977) IAU Circular No. 3051.
- Elliot, J. L., Dunham, E., and Mink, D. (1977a) *Nature*, **267**, 328.
- Elliot, J. L., Dunham, E. and Mink, D. (1977b) *Bull. Am. Astron. Soc.*, **9**, 498.
- Elliot, J. L., Dunham, E., Wasserman, L. H., Millis, R. L. and Churms, J. (1978) *Astron. J.*, **83**(8), 980.
- Elliot, J. L., French, R. G., Frogel, J. A., Elias, J. H., Mink, D. and Liller, W. (1980), Center for Astrophysics, Preprint series No. 1407.
- Elliot, J. L. (1981) in Uranus and the outer planets (IAU/RAS Colloquium No. 60 (G. Hunt, ed.), Cambridge University Press.
- Goldreich, P. and Tremaine, S. (1978), *Icarus*, **34**, 227.
- Goldreich, P. and Tremaine, S. (1980), *Astrophys. J.*, **241**, 425.
- Hénon, M. (1981), *Nature*, to be published.
- Klemola, A. R. and Marsden, B. G. (1977), *Astron. J.*, **82**, 849.
- Lecacheux, J. (1980) (Journées Scientifiques de la S.F.S.A.), *le Journal des Astronomes Français*, November 1980.
- Millis, R. L., Wasserman, L. H. and Birch, S. (1977), *Nature*, **267**, 330.
- Millis, R. L. and Wasserman, L. H. (1978), *Astron. J.*, **83**, 993.
- Nicholson, P. D., Persson, S. F., Matthews, K., Goldreich, P. and Vengebaner, G. (1978), *Astron. J.*, **83**(10), 1240.

# RCW 58: A Remarkable HII Region Around a WN 8 Star

M. C. Lortet and G. Testor, Observatoire de Meudon, and L. Deharveng, Observatoire de Marseille

In the course of a programme of detailed study of galactic ring nebulae around Wolf-Rayet stars, we obtained an  $\text{H}\alpha$  photograph,  $\text{H}\alpha$  interferograms and Boller and Chivens spectrograms of the H II region RCW 58 (Rodgers *et al.* 1960).

The  $\text{H}\alpha$  photograph is reproduced in Figure 1. The overall shape, as was known previously (Smith, 1968), is a ring centered on the WN 8 star HD 96548<sup>1</sup>. However, the nebula is remarkable for its clumpiness, the presence of large scale curls to the south, and above all the existence of radial features never observed for any other H II region.

The spectrograms indicate a relatively low degree of ionization, electron densities in the range 200 to 500  $\text{cm}^{-3}$ , and large variations of the line intensity ratio of  $[\text{S II}]\lambda\lambda 6717-6731/[\text{N II}]\lambda 6584$  over the nebula.

The radial velocity field, obtained from  $\text{H}\alpha$  interferograms, is complex; different clumps display different velocities, from about  $-60 \text{ km s}^{-1}$  to  $+60 \text{ km s}^{-1}$ . On the spectrograms, the  $[\text{N II}]\lambda 6584$  and  $\text{H}\alpha$  lines are tilted, and even split; the velocity difference between the two components reaches  $100 \text{ km s}^{-1}$  in the direction of a low brightness central region. This behaviour is reminiscent of those observed for NGC 6164-5 and M1-67<sup>2</sup>,

two nebulae formed of condensations ejected respectively by an O6f and a WN 8 star.

The complexity of the radial velocity field does not allow any estimate of a kinematical distance for RCW 58. If its central star is a typical massive WN 8 star ( $M_v \approx -7.0$ , Van der Hucht *et al.*, 1981), its spectroscopic distance is about 4 kpc.

Moffat and Isserstedt (1980) showed recently that the central star displays small periodic radial velocity variations; this may indicate the existence of a compact companion, so that the star would be a second-generation Wolf-Rayet star during the evolution of a binary system. This assumption is consistent with the large distance of the star from the galactic plane ( $z = 333 \text{ pc}$  for  $D = 4 \text{ kpc}$ ) which could result from the ejection of the system when the primary star exploded as a supernova. Under this assumption, the spatial motion of the

<sup>1</sup> HD 96548 = number 40 in the Catalogue of Wolf-Rayet stars by Van der Hucht *et al.* (1981) = MR 34 in Roberts (1962).

<sup>2</sup> M1-67 in the catalogue of Minkowski (1946) = Sh2-80 in the catalogue of Sharpless (1959); the  $\text{H}\alpha$  radial velocity fields of NGC 6164-5 and M1-67 were obtained respectively by Pismis (1974) and Pismis and Recillas-Cruz (1979).

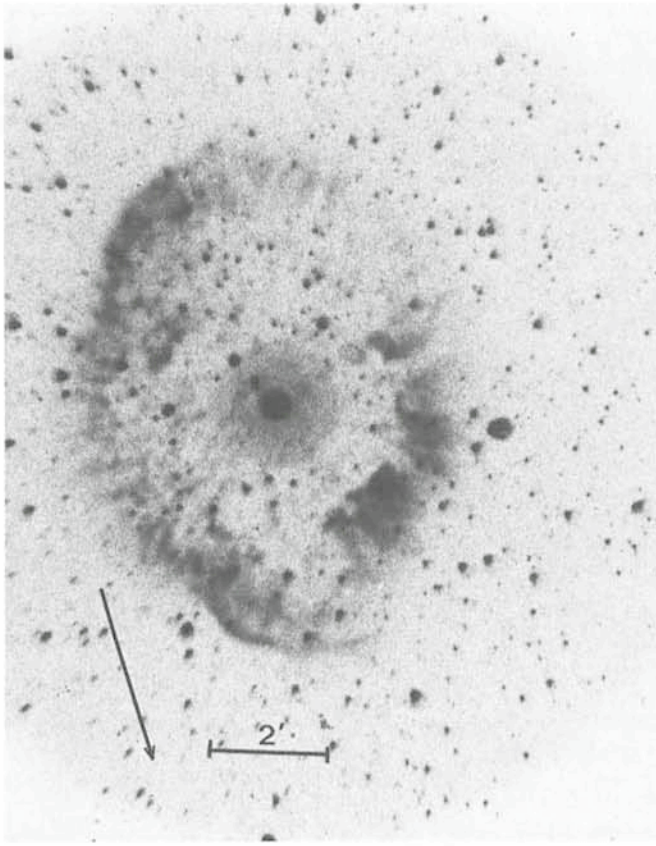


Fig. 1:  $H\alpha$  monochromatic photograph of RCW 58 (plate taken by G. Tenorio-Tagle and L. Deharveng). The device used is the "focal reducer" attached at the Cassegrain focus of the 152-cm telescope at La Silla (aperture ratio  $F/1$ , exposure time 30 min, baked Kodak IIIa-F emulsion). The arrow indicates the direction of decreasing galactic latitude.

system may be as large as  $100$  to  $200 \text{ km s}^{-1}$ . As no high radial systemic velocity is observed (the N IV line  $\lambda$  4058, with  $V_R = -16 \text{ km s}^{-1}$ , may have a velocity close to the systemic velocity, Moffat and Seggewiss, 1979), the motion may be nearly perpendicular to the line of sight. Its expected magnitude, about  $5$  to  $10 \cdot 10^{-3}$  arcsec per year, makes it detectable by the Hipparcos experiment to be launched in 1986 by ESA. The direction of the motion is expected to be nearly perpendicular to the galactic plane towards negative latitudes, as indicated on Figure 1.

Current work is going on in order to check the suggestion made by Chu (1980, 1981) that RCW 58 is primarily made of discontinuous ejecta from the central star, and to elucidate the process of formation of the southern curl and the radial filaments.

## References

- Chu, Y. H.: 1980, *Bull. Amer. Astron. Soc.* **12**, 842, and preprint.  
 Chu, Y. H.: 1981, Submitted to *Ap. J.*  
 Minkowski, R.: 1946 *Publ. Astron. Soc. Pac.* **58**, 305, table I.  
 Moffat, A. F. J., Isserstedt, J.: 1980, *Astron. Astrophys.* **91**, 147.  
 Moffat, A. F. J. Seggewiss, W.: 1979, *Astron. Astrophys.* **77**, 128.  
 Pismis, P.: 1974, *Rev. Mexicana de Astron. Astrof.* **1**, 45.  
 Pismis, P., Recillas-Cruz, E.: 1979 *Rev. Mexicana de Astron. Astrof.* **4**, 271.  
 Roberts, M. S.: *Astron. J.* **67**, 79.  
 Rodgers, A. W., Campbell, C. T., Whiteoak, J. B.: 1960, *M.N.R.A.S.* **121**, 103.  
 Sharpless, S. L.: 1959, *Ap. J. Suppl.* **4**, 257.  
 Smith, L. F.: 1968, in *Wolf-Rayet Stars*, p. 41, Proceedings of a Symposium held at the joint Institute for Laboratory Astrophysics, National Bureau of Standards, Boulder, Colorado (eds. K. B. Gebbie et R. N. Thomas).  
 Van der Hucht, K. A., Conti, P. S., Lundström, I., Stenholm, B.: 1981, *Space Sci. Rev.*, **28**, 227.

# Installation and First Results of the Coudé Echelle Spectrometer

Daniel Enard, ESO

## Introduction

The Coudé Echelle Spectrometer was installed in the 3.6-m telescope building in November and December 1980.

Despite several unexpected difficulties—like the necessity of the replacement of the granite table supporting the monochromator, which arrived broken into three pieces, and the astonishing discovery that the wall paint of the coudé room was slightly fluorescent—the instrument was assembled and pre-tested. Unfortunately, and because of lack of time, the final adjustment and first improvement of the software in the light of the first practical observations could not be done during this period. It is only in May 1981 that the first test observations were done with the active collaboration of E. Maurice and P. E. Nissen.

## The Instrument

The main characteristics are summarized in Table 1. The CES has already been described (D. Enard, *The Messenger* No. 11, Dec. 1977) and at the 1978 Trieste conference (D. Enard and J. Andersen, 4th Colloquium on Astrophysics,

Table 1. – CES CHARACTERISTICS

- Resolving power: optimal 100,000 (FWHM of instrumental profile)
- Spectral range: 3600–11000 Å
- 2 separate optical paths optimized for:
  - Blue  $3600 < \lambda < 5500$
  - Red  $5000 < \lambda < 11000$
- Modes:
  - Scanner single/double pass:
    - Max scanning frequency 5 Hz
    - Detector PMT QUANTACON
  - Multichannel:
    - Camera  $F/5$ , dispersion about  $1.2 \text{ Å/mm}$
    - Detector – Reticon RL 1872 F
      - CCD or photon counting device (not yet determined)
- Dispersive element:
  - $200 \times 400 \text{ mm}$  echelle grating; 79 grooves/mm, blazed at  $63^\circ 26'$
- Order separation achieved with a prism monochromator

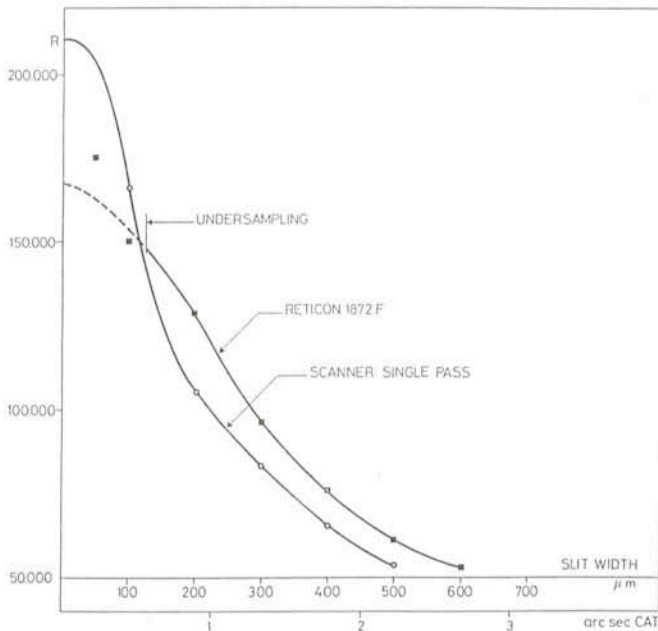


Fig. 1: "Slit function" of the CES. These curves indicate the resolving power versus the slit width. The resolution criterion is the full width at half maximum (FWHM) of the instrumental profile measured with a narrow laser line. From these curves one can immediately derive that the combination CAT-CES is well optimized for resolving power of the order of 100,000.

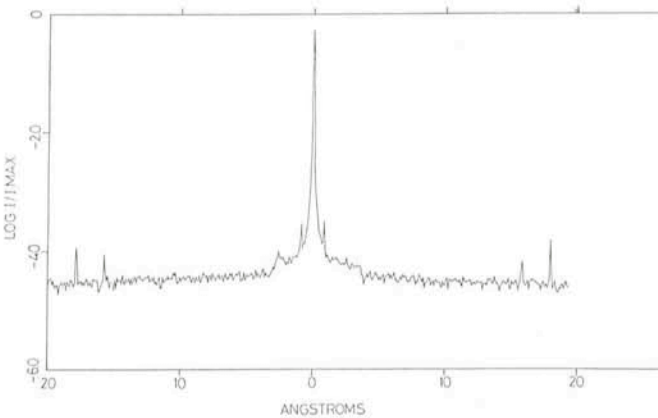


Fig. 2: Instrumental profile obtained by scanning a laser line. Rowland ghosts, symmetrical with respect to the line disappear when working in double pass.

Trieste, July 1978). At that time the instrument was still being designed. However, the characteristics have not changed significantly, except, unfortunately, the faint-object multi-channel detector (a Digicon) which became unavailable, so that the only multichannel detector available now is a Reticon. This detector, although it gives excellent results, is of course limited by its read-out noise.

The user's interface has been designed to be as far as possible friendly to observers, above all to visiting astronomers who may not be totally familiar with a computer-controlled instrument and the ESO image-processing system.

Achieving a high degree of automation implies, of course, complex software and a delicate analysis of the functioning of the instrument. For instance, setting the instrument basically requires that the observer types in the central wavelength and the resolution desired. However, the programme has to determine the correct order of the échelle grating, the position of the grating and of the pre-disperser prism, the slit width and—in the case of the scanner—the parameters of the scan from the desired length of the spectrum that the observer must also introduce. This apparently simple operation implies that a considerable number of parameters are previously determined and introduced into the programme.

The observer has a complete freedom to organize his sequence of observations: spectral and photometric calibration, dark signal and object measurement are all considered equivalent by the system and recorded on a disk and a mag tape chronologically. However, by placing the result of the calibrations into appropriate buffers before observing the object, it is possible to obtain a limited but immediate reduction of the data, so that the observer can immediately appreciate the quality of his observation.

## The Telescopes

In principle, the CES can be fed by either the 3.6-m or the 1.4-m Coudé Auxiliary Telescope. The coudé focus of the 3.6-m is not yet operational so that only the CAT can presently be used. Surprisingly, the seeing of that telescope—despite the very long optical path—seems to be excellent. A typical resolving power of 100,000 corresponds to a slit of 1.2 arcsec and a slit throughput of the order of 70% has been obtained during roughly 70% of the nights. However, this figure, being based on the first preliminary observations, should be taken cautiously. Because the 3.6-m coudé operation is not very efficient, ESO is considering as an alternative the possibility of coupling the CES to the prime focus of the 3.6-m with a fiber optics instead of using the 5-mirror coudé train.

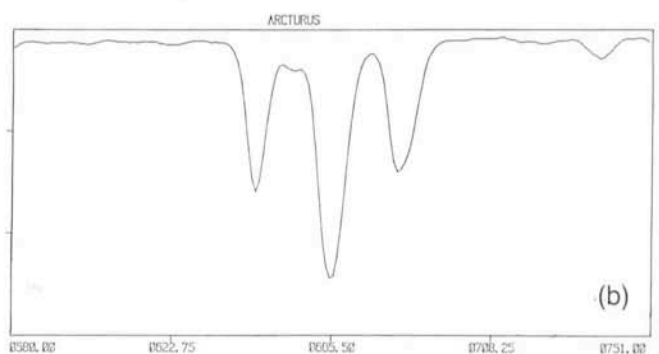
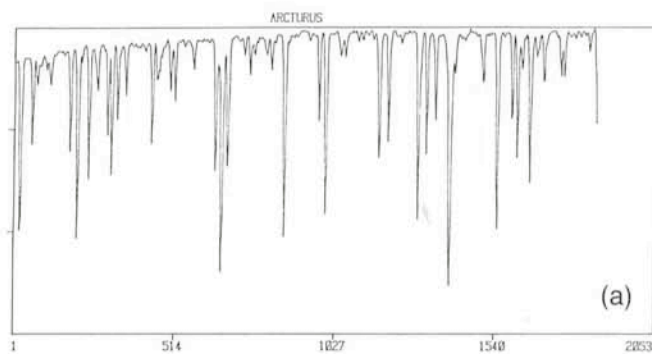


Fig. 3: (a) Spectrum of Arcturus. It covers 50 Å (6085–6135 Å) at a resolution of 60 mÅ. A signal-to-noise ratio better than 1,000 is obtained in 200 seconds. (b) Expansion of the same spectrum showing the Ca lines around 6102 Å.

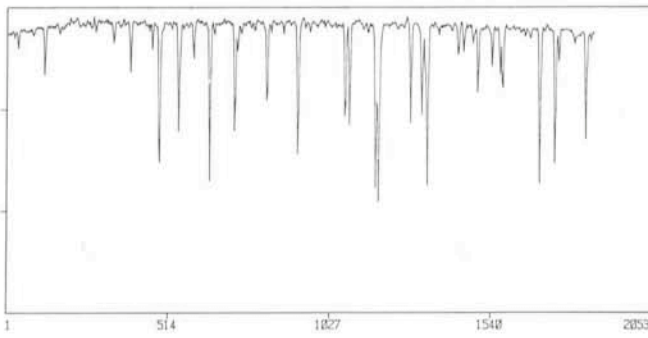


Fig. 4: Spectrum of Nu Indus at 5135 Å. The spectrum covers 42 Å (5114–5156 Å) and a signal-to-noise ratio of 120 is obtained on this 5.2 magnitude star after 30 minutes at a resolution of 60 mÅ.

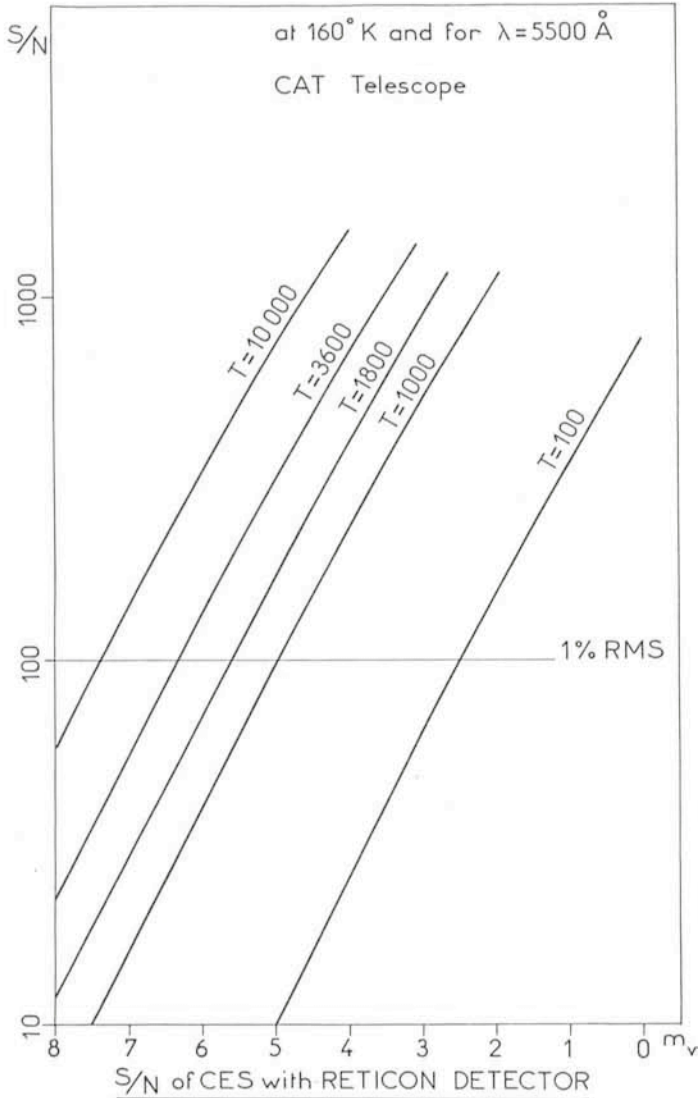


Fig. 5: Efficiency curves of the CES with a Reticon. They give the signal-to-noise ratio one can expect for a given integration time and under reasonably good seeing conditions at 5500 Å. For lower wavelength the Reticon sensitivity decreases fastly and corrections must be applied.

### First Results

(a) *Resolution.* Results obtained in the laboratory have been confirmed. Effective resolution (FWHM of instrumental profile) versus slit width is shown by Figure 1 for the red path.

Resolution in the blue is slightly worse because of the poor quality of the pre-disperser prism. It is foreseen to replace that prism in the near future. Figure 2 illustrates the extremely low level of stray light, a result of the high quality of the échelle grating and of the pre-disperser which introduces into the spectrometer a minimum of light.

(b) *Observations of Arcturus.* This very bright star has been observed in several wavelengths and provides an easy comparison with other observations. Figure 3 shows the spectrum obtained around 6110 Å with the Reticon, and an expansion of the same spectrum showing the Ca lines around 6102 Å. Results obtained with the scanner are very similar in quality to those obtained with the Reticon. Difference in depth of absorption lines was found to be less than 1%. Efficiency of the Reticon is however much higher because of simultaneous multichannel integration and high quantum efficiency.

(c) *Observation of Fainter Objects.* In order to determine the limit of the instrument, a number of objects up to magnitude 6.5 have been observed. As an example, Figure 4 shows a spectrum of NU INDUS ( $V = 5.22$ ) obtained in the 6102 Å region with an integration time of 30 minutes.

The efficiency curves of Figure 5 have been calculated taking into account the average good seeing obtained with the CAT and the real noise level of the Reticon. These curves are in good agreement with practical observations so that they can be used as a guide for determination of observing time. However, many parameters have also to be considered such as:

- Relative quantum efficiency of the Reticon. (For example, the loss of sensitivity for H and K lines is nearly one magnitude.)
- Relative distance from the blazed wavelength of one order. The corresponding loss of efficiency can be as high as 50% and is calculated by the programme for the central wavelength.
- Actual seeing and slit width.

### Present Status and Availability

The instrument is now operational at La Silla. However a few functions like the setting of the slit widths and the selection of neutral densities for the calibration are still manual. Full control from the main console is expected to be installed during the first half of 1982. The CES will be offered to visitors from January 1st, 1982.

Further improvement of the instrument will be considered in the near future. A very promising development would be the installation of a CCD detector possibly coupled to an F/3 camera. The resolution would be reduced to 60,000 but a gain of 3 to 4 magnitudes is to be expected.

## New Large Interference Filters for the 3.6-m Triplet

D. Enard and M. Tarenghi, ESO

The triplet adaptor (see *The Messenger* No. 16, page 26 for a description by M. Ziebell) was put into operation in November 1979 and since then it has been used regularly both with large 240 × 240-mm plates and with the 40-mm McMullan electronographic camera (*The Messenger* No. 19, p. 33).

In the meantime new photographic possibilities at the prime focus of the 3.6-m telescope have been implemented. Thanks

Table 1. – Characteristics of the new interference filters now available with the triplet corrector

Nominal mean wavelength (Å)	6748	6577	6500	5024	4880
Mean effective wavelength at the 3.6-m Prime Focus (Å)	6735	6565	6488	5014	4871
Bandpass (Å)	110	58	100	100	110
Variation of central wavelength over $\varnothing$ 220 mm (Å)	14	10	18	10	8
Variation of BW over $\varnothing$ 220 mm (Å)	1	0.5	2	4	2
Peak transmission (%)	91	90	96	92	76.5
Blocking T < 0.1 %	0.3–1 $\mu$ m	0.3–1 $\mu$ m	0.3–1 $\mu$ m	0.3–0.88 $\mu$ m	0.3–1 $\mu$ m

to improvements of the dark-room it is possible not only to obtain a better development of the large-format plate but also to make use of IV N plates sensitized with the silver nitrate technique.

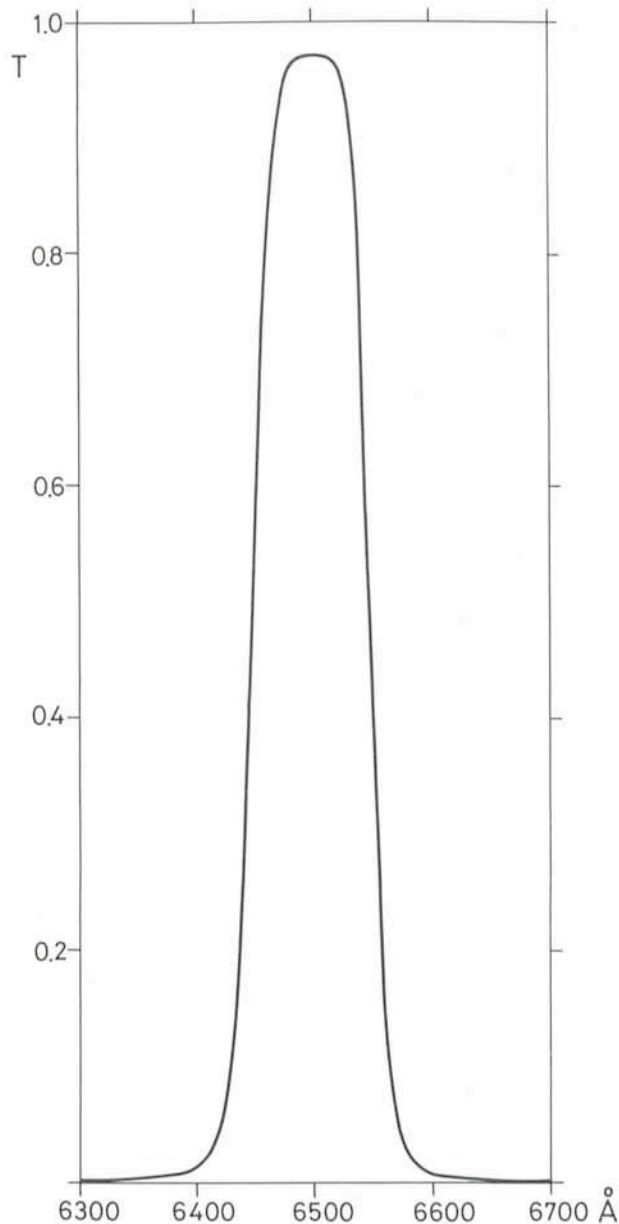


Fig. 1: Transmission curve of the  $H_{\alpha}$  "continuum" filter for the triplet corrector.

Two of the four available large-field ( $\sim 1^{\circ}$ ) transmission gratings have been used with complete satisfaction by the visiting astronomers.

The 80-mm McMullan electronographic camera has been tested, showing good mechanical and electronic performances but an unacceptable quality of the tube. A new tube will arrive soon. Finally a Racine wedge is in the process of being ordered.

A set of large interference filters have recently been developed for use at the 3.6-m telescope and the triplet corrector. These filters are 230  $\times$  230 mm large, the useful area being however limited to a circle of 220 mm in diameter.

They are multilayer filters and they exhibit the typical band shape of this type of filters with steep side slopes, an example of which is given in Figure 1. Despite their very large size, the central wavelength varies by less than 20% of the bandpass over the surface, and the bandpass is practically constant.

For anyone aware of the difficulties of making large interference filters there is no doubt that this represents a great achievement and the present ultimate state of the art, thanks to the talent of Dick Bennett from Andover Corp. Moreover, the optical quality is kept excellent—no detectable degradation of image quality being noticed—and the two external faces are coated with a hard and cleanable anti-reflexion coating. Transparency is therefore improved and intensity of ghost images reduced.

Table 1 gives the main characteristics of the filters which are now available at La Silla.

Because of their size it was not possible to measure the performances of these filters on a classical double-beam spectrophotometer. A new type of instrument has been used.

This instrument has been developed to measure the absolute transmission or reflexion of optical elements whatever their size and optical power. It is therefore possible to measure absolute efficiency of mirrors, lenses and even gratings up to 60 cm wide. A new set of interference filters has also been developed for use with the 40-mm and 80-mm MacMullan cameras. They correspond to the u, v, b, y' bands of the Strömrgren photometric system and come in addition to the present glass filters (Table 2). Their main advantage is that red leak beyond 6500 Å inherent to glass filters is totally suppressed.

Their useful diameter is 110 mm and variations over the surface are negligible with respect to the bandwidth.

The first picture obtained in a test night is shown in Figure 2; it shows the Orion nebula. The print presented here has been obtained by making use of the masking technique by C. Madsen (*The Messenger* No. 26, p. 16). The filamentary structure is well visible both in the central region and in the external envelope.

Table 2. – Characteristics of the u, v, b, y' interference filters now available with the McMullan camera and the 3.6 m telescope

Nominal mean wavelength ( $\text{\AA}$ )	3457	4090	4708	5771
Mean wavelength corrected for 3.6-m Prime Focus ( $\text{\AA}$ )	3443	4078	4700	5760
Bandpass ( $\text{\AA}$ )	365	156	180	186
Peak transmission (%)	57	63	82	94.5
Blocking T < 0.1 %	0.3–1 $\mu\text{m}$	0.3–1 $\mu\text{m}$	0.3–1 $\mu\text{m}$	0.3–0.84 $\mu\text{m}$

The second example of use of the interference filter is showing NGC 300 (Fig. 3). The heliocentric radio velocity of NGC 300 being only 145 km/s, the  $H_{\alpha}$  filter is almost centered on the  $H_{\alpha}$  emission of the galaxy. A comparison between the blue and the  $H_{\alpha}$  images gives a clear picture of the location and structure of the numerous H II regions.



Fig. 2: The Orion nebula. One hour exposure on a 098–04 emulsion behind the  $H_{\alpha}$  interference filter at the prime focus of the ESO 3.6-m telescope.

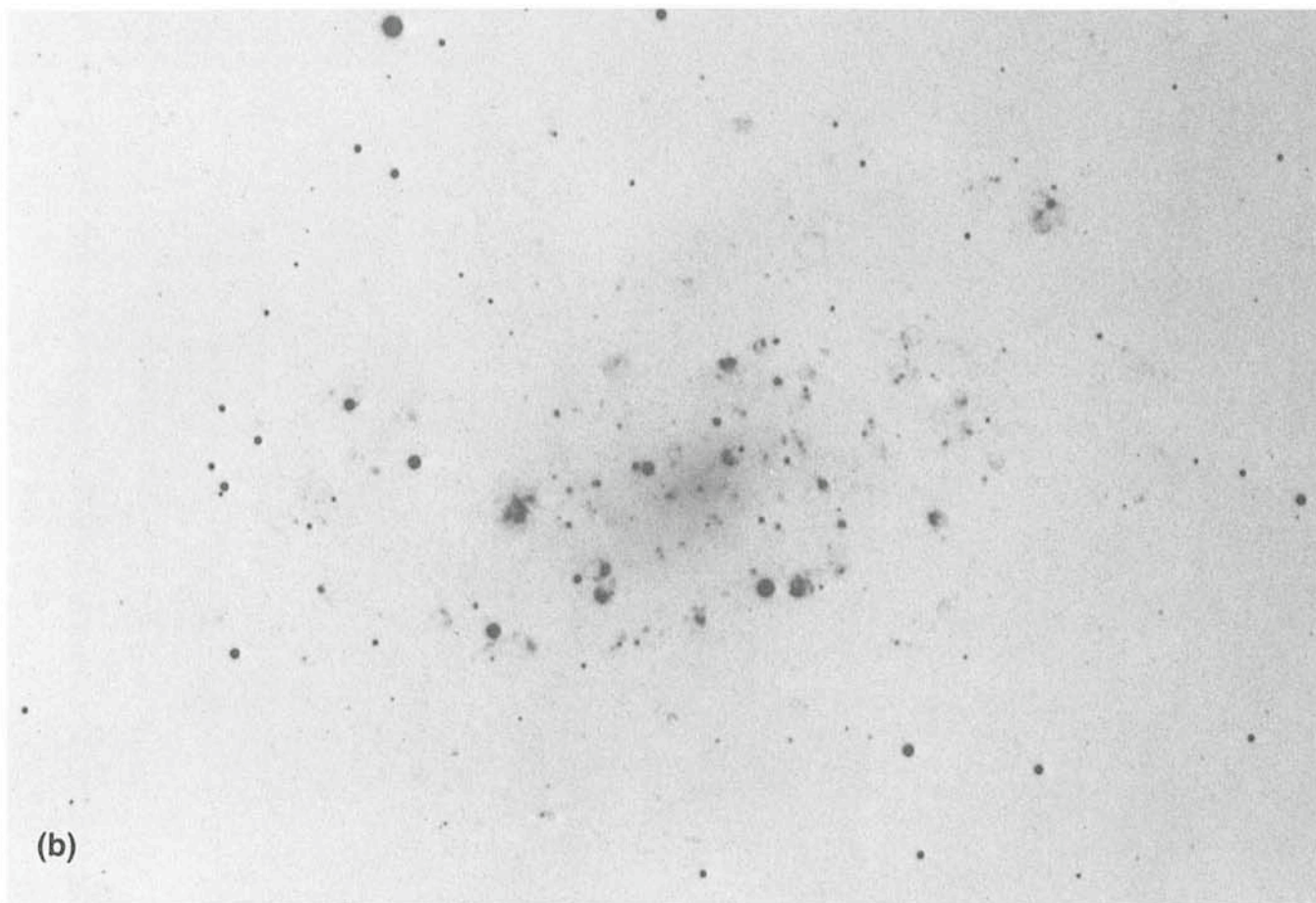
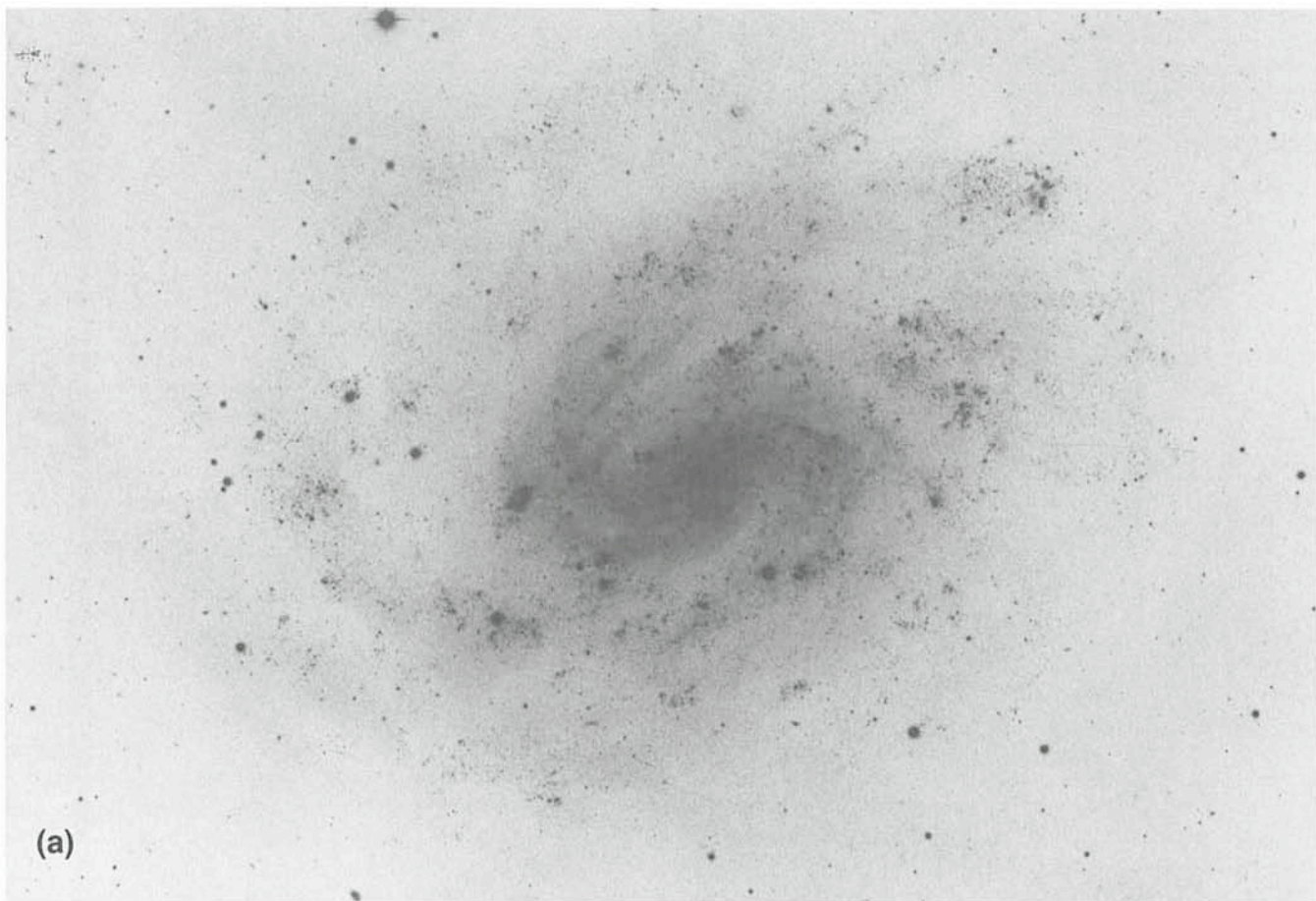


Fig. 3: The Sc galaxy NGC 300: (a) A 10-min exposure, with the blue corrector, on a 11a-O baked plate, without filter; (b) a 1<sup>h</sup> 30<sup>m</sup> exposure, with the red corrector, on a 098-04 emulsion behind the H<sub>α</sub> interference filter.

# Discovery of a Very Fast Optical Activity in the X-Ray Source GX 339–4

Ch. Motch, ESO

S. A. Ilovaisky and C. Chevalier, Observatoire de Meudon, France

## Introduction

Most galactic X-ray sources are compact objects (white dwarfs, neutron stars and maybe black holes) in binary systems. Matter coming from a normal companion star is driven onto the surface of the compact object where the release of gravitational energy powers the X-ray emission. The energy emitted at X-ray wavelengths ranges from  $10^{35}$  to  $10^{38}$  erg/s and a mass transfer rate of typically  $10^{-11}$  to  $10^{-8} M_{\odot}$ /year is enough to explain the X-ray luminosity. In most of the cases an accretion disk is formed around the compact object due to the angular momentum carried by the matter escaping the companion star. Recent investigations have shown that the accretion disks can be very large and that the heating of their surface by the X-rays emitted by the central source can make them very luminous.

X-ray astronomers usually distinguish between massive and low-mass X-ray binaries. In the massive X-ray binaries, the companion of the compact object is a giant hot star (OB type with surface temperature of 20,000–30,000° K). Its mass (10 to 20  $M_{\odot}$ ) is large compared to the mass of the compact object (1–2  $M_{\odot}$ ), and its optical–UV luminosity is  $\sim 10^{38}$  erg/s. In this case, the optical emission from the disk itself (some  $10^{36}$  erg/s) is difficult to detect. Optical variability is small and essentially due to the changes of aspect with orbital motion of the tidally distorted companion star. In the low-mass systems, the stellar companion has a mass equal to or less than the X-ray source yielding a very different picture. The disk becomes visible and often dominates the optical emission of the system. This kind of system is the most suitable to study the accretion disks, provided that it is possible to distinguish clearly the contributions of other likely sources, as the X-ray heated hemisphere of the companion and the surroundings of the X-ray source itself.

## Variability

An almost universal feature of X-ray sources is the variability of their X-ray flux. Time scales of variations ranging from years to milliseconds are observed. Strictly periodic variabilities are common and are caused by three mechanisms:

- The orbital motion (a few hours to a few days).
- The rotation of the compact object (a few seconds to a few minutes). If the neutron star or the white dwarf has a strong enough magnetic field, matter will be driven along magnetic field lines down to the polar cap where the X-ray emission will take place. If the compact object rotates, an earth observer will then see X-ray pulsations due to the periodic crossing of the line of sight by the X-ray beam.
- The precession of the disk can shadow periodically the X-ray source (about 1 month).

Unperiodic random variability can also occur on a wide range of time scales. Bursts of some tens of seconds can be explained by instabilities in the accretion process or thermonuclear flashes on the surface of the neutron star. Some sources like Sco X-1 display a variability on time scales of minutes which is not quite well understood. Long-term (months to year) variations reflect in most cases changes in the accretion rate.

Three remarkable sources, Cyg X-1, GX 339-4 and Cir X-1 show very peculiar random variability. Their time behaviour is

highly erratic on a time scale of seconds, and flares as short as some milliseconds have been observed. This activity is usually mathematically described by a shot-noise random process, in which the time-dependent flux is the result of the superposition of elementary narrow pulses randomly distributed in time. Unfortunately, this description, which is useful to compare the activity of different objects, is not very helpful to understand the underlying physics. Several mechanisms have been proposed: rotating hot spot in the inner parts of the accretion disk, hydrodynamical instabilities, transient magnetic structure, etc. But in our present state of knowledge, it is impossible to rule out one of these possibilities. These three X-ray sources have another common feature: the X-ray intensity has two preferred states, high and low. During the high state the spectrum has an excess of soft X-rays ( $< 3$  keV) with respect to the low state. Theoretical models, built under the assumption that the compact object is a black hole (as it is thought to be the case for Cyg X-1), explain this bimodal behaviour as due to changes in the density, size and plasma properties of the innermost parts of the accretion disk which are thought to be, in this case, the X-ray emitting regions.

## Optical Observations

The stellar companion of Cyg X-1 is massive and optically dominates the system, making the accretion disk hardly visible in the optical. Optical studies of the two other members of this class revealed a continuous spectrum with emission lines, but failed to detect any stellar absorption lines. They also showed that the brightness of the optical counterpart is variable by 2–3 magnitudes.

These two pieces of evidence indicate that they must be low mass binaries. Cir X-1 is very far away and absorbed in the optical ( $B \sim 20$ ) making optical studies rather time-consuming. GX 339-4 is brighter ( $V = 16$  to 18) and is thus a better choice. It was indeed on our target list in March 1981, during an observing run at the 3.6-m at La Silla. At the same time, J. Hutchings, A. Cowley and D. Crampton, visiting astronomers at Cerro Tololo, had planned to take some spectra of this object, but could not find the star anymore. Some days later, on March 6, we pointed the 3.6-m telescope and had the same surprise. The object had disappeared from the sky. The following night, a Schmidt plate was taken by M. Pizarro.

The object was found to be in an unreported faint state ( $B \geq 21$ ). We warned our Japanese colleagues who maneuvered the X-ray satellite HAKUCHO and found that on April 7, the X-ray flux of GX 339-4 was below the limit of detection. Such large variations in the X-ray and optical fluxes are not unusual among X-ray transients and novae. They are thought to be due to an increase of matter accretion and thus of X-ray emission which in turn heats the companion star and the recently built accretion disk, producing the optical brightness jump. This confirmed that GX 339-4 is a low-mass system with most of the light coming from X-ray heating.

During another run at the 3.6-m telescope in infrared on March 24, we naturally pointed the telescope toward GX 339-4. We had another surprise; the star was back to a very bright state ( $V = 15.4$ ), also unreported in the literature (see Fig. 1).

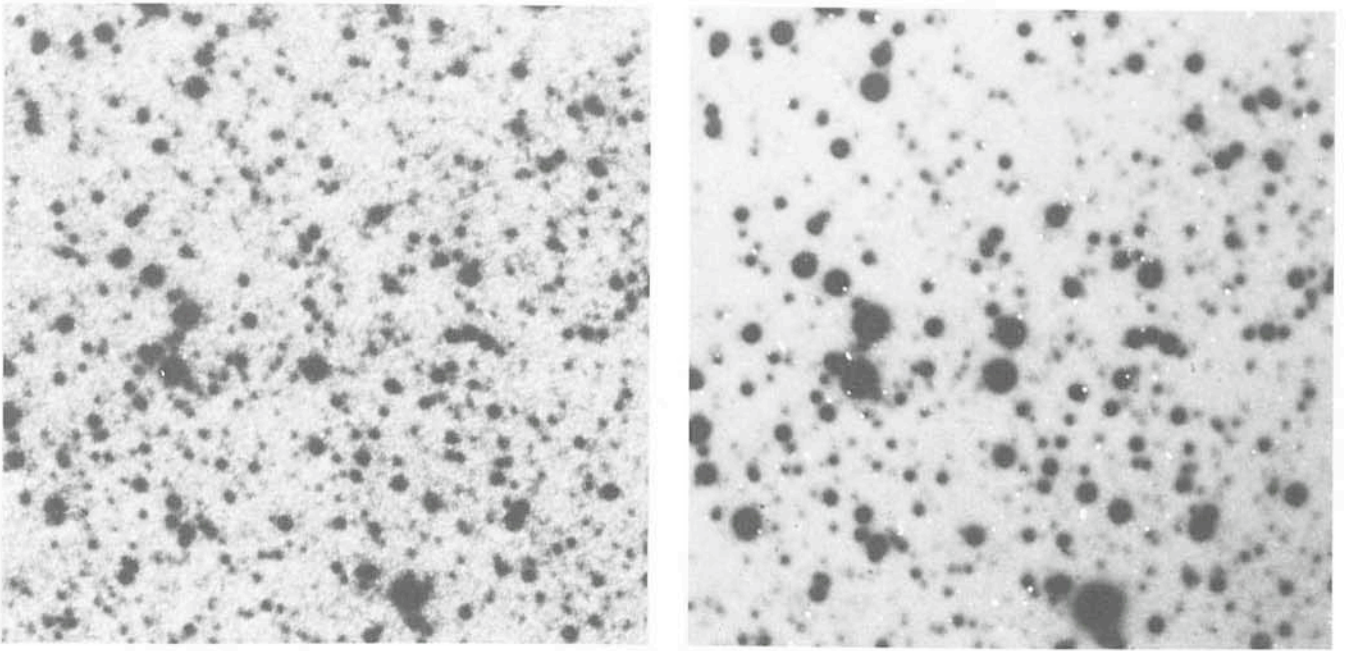


Fig. 1: GX 339-4 field with the object at minimum (left) and at maximum (right). Left: enlargement from a 1-m ESO Schmidt plate (taken by G. Pizarro) in the blue (IIIa-J + GG385 filter) of a 90-min exposure taken on March 1981. Right: enlargement from a 3.6-m ESO prime-focus plate taken with the Triplet Adapter and the 4-cm McMullan electronographic camera with a B filter. A 90-min exposure, taken by H. E. Schuster, on 1 June 1981. The object is at the center. North is at the top, East to the left. The fainter star immediately to the NE of GX 339-4 has  $B = 19.5$ . The almost equally bright star farther South has  $B = 15.9$ .

We undertook classical photometry and were a bit disappointed by the lack of accuracy of the measurements. The dispersion of the single integrations were far too large for the number of photons counted. We thus decided to further investigate the time behaviour of GX 339-4 making fast photometry observations.

On May 28 and 29, we used the 1.5-m Danish Telescope equipped with the Danish double beam (star/sky) photometer.

We used the full response of two RCA 31034 GaAs red sensitive tubes. The star was kept centered in a 9 arcsecond diaphragm by the auto-guider system. Integration time was 10 milliseconds. These observations revealed soon the unprecedented activity of the optical flux (see Fig. 2). It took us some time to become convinced of its reality. The same observations made from time to time on an anonymous field star of similar brightness did not show any particular activity. The data from

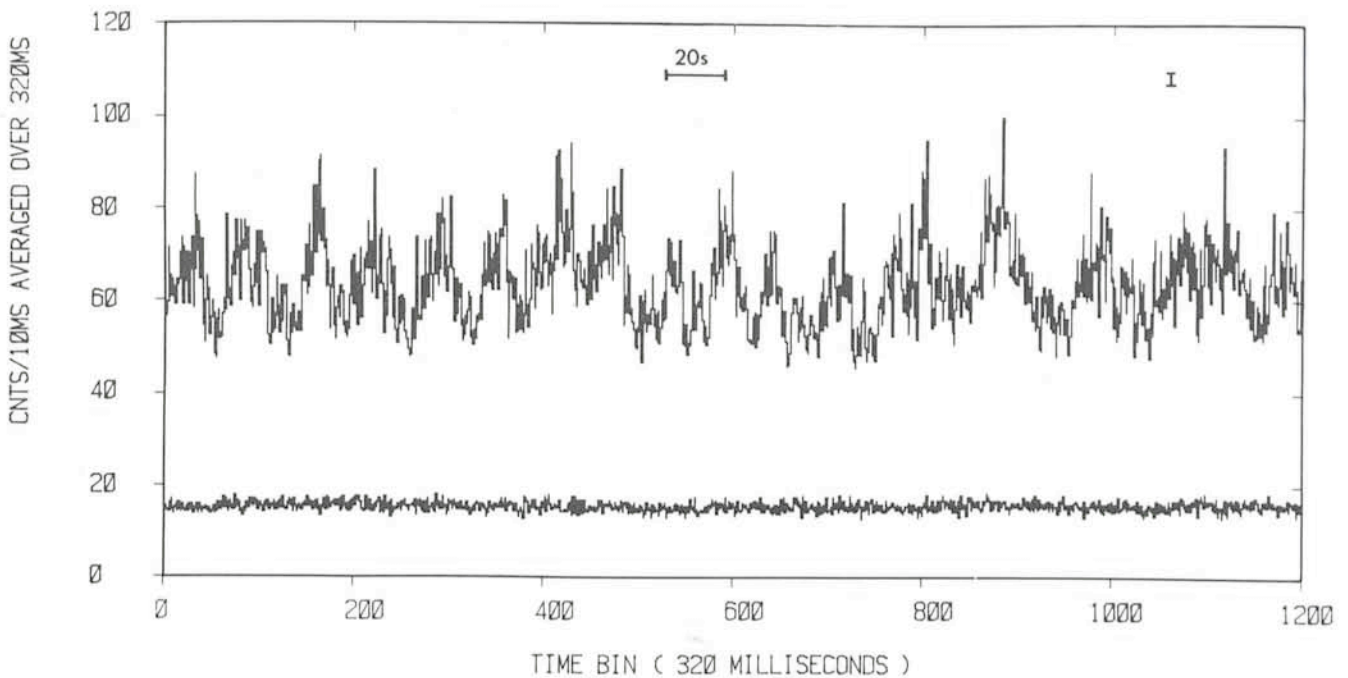


Fig. 2: A part of the optical lightcurve of GX 339-4 in white light (3400–9000 Å). 10 millisecond data have been averaged in 320 millisecond bins. The sky background recorded by the other photometric channel is also shown. Typical error bar is indicated. The high-amplitude, 20-second quasi-periodic oscillations are clearly visible as well as the large flaring activity.

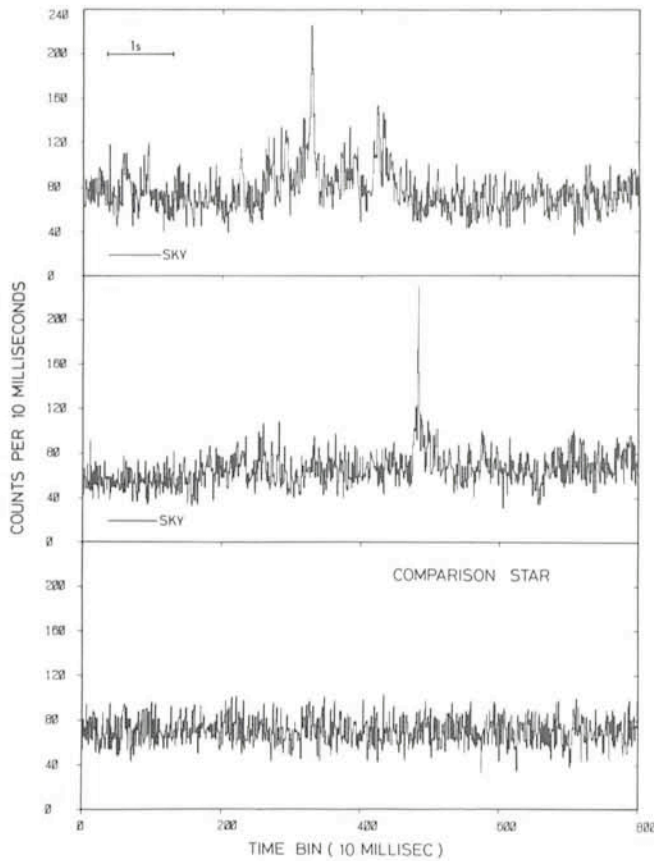


Fig. 3: A sample of very short (10 to 30 milliseconds width) optical flares from GX 339-4. Data are shown with 20 millisecond time bins. The companion star data (of same integrated brightness as GX 339-4 in the wavelength range 3400–9000 Å) give an estimate of the actual noise. Sharp flares may occur alone or accompanied by other small ones. Two series of flares ending with a large one are shown (bottom).

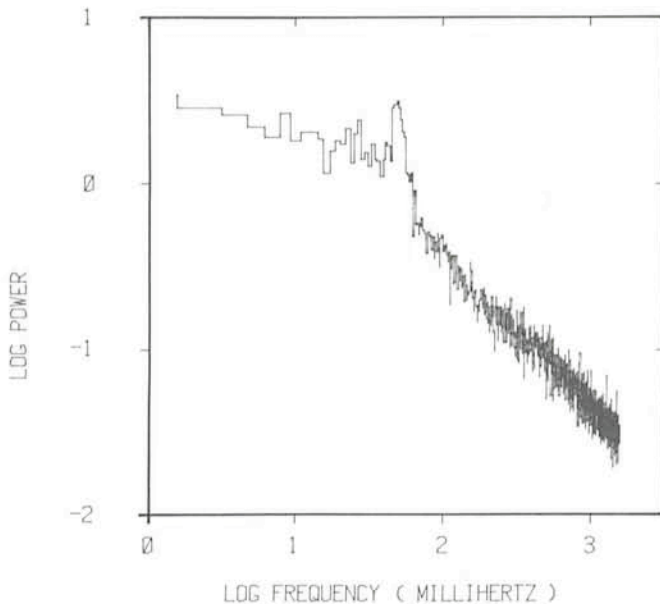


Fig. 4: The average Fourier Transform of GX 339-4 computed on data averaged in 320 millisecond bins and plotted in log/log scale. The power spectrum is almost flat for frequencies below 0.05 hertz ( $P = 20$  seconds) and displays a  $1/f$  slope at high frequencies. The quasi-oscillations at  $P = 20$  seconds clearly appear as a hump located at the knee frequency of the power spectrum.

the other photometer channel (sky) were also normal and finally weather conditions and seeing were excellent.

The large fluctuations clearly visible on Figure 2 were readily found to be 20 second quasi-oscillations with a full amplitude of 30 to 40%. Secondly, a careful look at the data stream with full time resolution revealed the presence of flares as short as 10 to 20 milliseconds, during which the flux of the object can be multiplied by a factor of 2 to 5! (see Fig. 3). In less than 3 hours of observations, we detected about 900 flares at a  $6\sigma$  level. Some large flares were accompanied by other smaller flares before and after, and some tend to show a decay of the total flux just after.

A statistical analysis of the data proved them to be consistent with a shot noise process. Few papers study the flaring activity of GX 339-4 and we had to compare mainly with the X-ray behaviour of Cyg X-1, also described in terms of shot-noise and widely studied. In fact, the resemblance is striking. The power spectrum shown in Figure 4 is very similar to that of the X-rays of Cyg X-1 reported by Nolan *et al.* (1981, *Astrophysical Journal* **246**, 494). They both show an almost flat part at low frequencies, a  $1/f$  slope at high frequencies and the knee frequency is the same in both cases. Finally, the only difference is the presence of the 20 seconds quasi-oscillation in the optical of GX 339-4.

Analysis of the auto-correlation function revealed the same decay times as for Cyg X-1. The striking resemblance between the time behaviour of the opticals of GX 339-4 and the X-rays of Cyg X-1, and the fact that, at the time of the optical observations, X-ray observations made with the Ariel 6 satellite (Ricketts, private communication) showed that GX 339-4 was in a low and flaring state, prove that X-ray and optical flares have close origin. However, the sharpness of the optical flares raises some problems. A 10-millisecond time structure implies a typical dimension of 3,000 km for the optically emitting region. Assuming a Rayleigh-Jeans spectrum for the optical emission and a distance of 4 kpc, the temperature of the emitting region is found to be  $5 \cdot 10^9$  °K. Such a high temperature cannot be due to X-ray heating, but is consistent with the electronic temperatures derived for the innermost X-ray emitting parts of the disk by theoretical models of Cyg X-1 in the low state. The optical flares probably come from this region, but the exact emitting mechanism (bremsstrahlung, cyclotron emission) is unknown.

The origin of the 20-second quasi-oscillations is not clearer. The fact that they have a mean frequency equal to the knee frequency common to GX 339-4 and Cyg X-1 indicates that the mechanism responsible for the quasi-oscillations is physically related to the one producing the random X-ray and optical flares. If the mechanism at work in GX 339-4 is similar to the one present in a dwarf nova during outbursts (nonradial oscillations of disk annuli), the large amplitude indicates that the disk is small and ring-shaped. A typical radius is 11,000 km, a size similar to the one derived from the flare time scales and consistent with the size of the outer cool parts of accretion disk models of Cyg X-1. However, instabilities of the very hot inner parts of the disk, theoretically described by Shakura and Sunyaev (1976, *Monthly Notices of the Royal Astronomical Society* **175**, 613) could also trigger the quasi-oscillations.

We have certainly witnessed during those three months the onset of mass transfer, and the reformation of an accretion disk. We plan to carry on optical studies of this very interesting object in order to see whether the remarkable time behaviour found at maximum light is also present when the star has a normal brightness and how it changes with X-ray state. Correlated optical and X-ray observations should give much insight on the physics of this peculiar class of X-ray source.

## IN MEMORIAM



### SONIA (1967–1981)

During a thundery evening, on May 13, 1967, a little female with fiery eyes and an independent character was born on La Silla. She was called Sonia. It was said that she was very pretty.

Coquettish until the end, she enjoyed her young life as a perfect courtesan. Later, perhaps as a result of the influence of her protector, H. E. Schuster, she became a paragon of virtue. Intelligent and discrete, she devoted her life to the Observatory where, on September 28, 1981, she passed away quietly. P.B.

En una noche tempestuosa, el 13 de mayo de 1967, una madre de costumbres tan evidentes como su nombre, dio a luz en La Silla a una perrita que en casi nada se parecía a su padre, Chocolate. Sin embargo, como él, se mantenía bien sobre sus cuatro patitas, el vientre algo bajo, pero firme. De su madre había heredado la pícaro mirada que no sería alterada por el peso de los años, y una cierta independencia de carácter desde ya muy pequeñita. Siendo bien bonita era también bastante coqueta. Y con el correr de los años, mientras su belleza se desvanecía, aumentaba su coquetería.

Fue bautizada "Sonia" por su padrino, Hans-Emil Schuster, quien tendría una determinada influencia sobre su existencia. En particular la hizo renunciar a sus actividades de cortesana que tanto agitaran su adolescencia. En efecto, era incalculable el número de galanes que no vacilaban en correr por el desierto para venir a solicitar los favores que ella no sabía rehusar. Pero una vez desterradas aquellas punibles actividades, demostraría una castidad casi ejemplar durante la última parte de su vida. Desde entonces no tenía más que a un compañero de juegos, el aristocrático Lord, un año mayor que ella, del cual la separaba todo, pero quien le aportaría una amistad sincera nacida de un mutuo respeto, y de una común necesidad.

Dotada de una inteligencia notable al servicio de su pereza, ladró bastante rápido en alemán, holandés y español, y obedecía en francés. Jamás gruñía sin premeditación y no levantaba la voz mas que cuando se le ordenaba, cosa rara en La Silla. Tenía horror de ser considerada como un animal de circo, no prestaba atención alguna a las zalamerías dispensadas por aquellos que buscaban halagar a su padrino. Fiel y silencioso testigo de todas las reuniones, consagró su vida al Observatorio entre la cúpula, su habitación y la cocina. ¿A cuántos astrónomos habra conocido? ¿Cuántas noches habrá pasado junto al telescopio? Hasta aquel 2 de septiembre de 1981 en el cual gastada y fatigada esta vieja solterona se dormiría para siempre en La Silla, antes de mucho sufrir. P.B.

## PERSONNEL MOVEMENTS

### STAFF

#### Arrivals

##### Europe

ZIEGLER Véronique (F), Administrative Clerk, 1.1.82  
KAZIMIERZAK Bohumil (B), Mechanical Engineer, 1.3.82

#### Departures

##### Europe

BERNARD Marie-Françoise (F), 31.1.82

### ASSOCIATES

#### Arrivals

##### Europe

WAMPLER Joseph (USA), 1.9.81  
SETTI Giancarlo (I), 1.1.82

##### Chile

IHLE Gerardo (NL), Mechanical Engineer, 1.2.82

#### Departures

##### Europe

KRUSZEWSKI Andrzej (PL), 8.2.82

##### Chile

ANGEBault Louis (F), Coopérant, 31.10.81  
BARBIER René (B), Fellow, 31.12.81

## ALGUNOS RESUMENES

### Información sobre vinchucas y la enfermedad de Chagas

*Con motivo del considerable aumento del número de vinchucas observadas en La Silla durante el verano pasado, el Director General de ESO solicitó al Prof. Hugo Schenone, Director del Departamento de Microbiología y Parasitología de la Universidad de Chile, de visitar La Silla para investigar la situación. A continuación damos un resumen de su informe.*

¿Qué son las vinchucas? Son insectos que pertenecen al grupo de los tratominos. Tanto los adultos como las formas juveniles se alimentan exclusivamente de sangre la cual obtienen al picar a diversos animales tales como mamíferos, aves y reptiles, incluso al hombre.

¿Cómo se reproducen y desarrollan las vinchucas? Las hembras fecundadas colocan sus huevos que miden alrededor de 1,5 mm de largo en lugares protegidos. De los huevos nacen las formas juveniles llamadas ninfas, las que a medida que crecen van mudando de piel hasta alcanzar el estado adulto. Los adultos, que por lo general son alados, tienen forma ovoidea, miden alrededor de 2 cm de largo, son de color negro o café oscuro y en su abdomen presentan manchas de color amarillento o rojizo dispuestas en forma alternada. Las formas juveniles o ninfas son de color plomizo o pardo, de aspecto terroso.

¿En qué países existen vinchucas? Prácticamente en todos los países del continente americano, excepto Canadá.

ESO, the European Southern Observatory, was created in 1962 to . . . establish and operate an astronomical observatory in the southern hemisphere, equipped with powerful instruments, with the aim of furthering and organizing collaboration in astronomy . . . It is supported by six countries: Belgium, Denmark, France, the Federal Republic of Germany, the Netherlands and Sweden. It now operates the La Silla observatory in the Atacama desert, 600 km north of Santiago de Chile, at 2,400 m altitude, where twelve telescopes with apertures up to 3.6 m are presently in operation. The astronomical observations on La Silla are carried out by visiting astronomers – mainly from the member countries – and, to some extent, by ESO staff astronomers, often in collaboration with the former. The ESO Headquarters in Europe are located in Garching, near Munich. ESO has about 120 international staff members in Europe and Chile and about 150 local staff members in Santiago and on La Silla. In addition, there are a number of fellows and scientific associates.

The ESO MESSENGER is published four times a year: in March, June, September and December. It is distributed free to ESO personnel and others interested in astronomy. The text of any article may be reprinted if credit is given to ESO. Copies of most illustrations are available to editors without charge.

Editor: Philippe Véron  
 Technical editor: Kurt Kjær

EUROPEAN  
 SOUTHERN OBSERVATORY  
 Karl-Schwarzschild-Str. 2  
 D-8046 Garching b. München  
 Fed. Rep. of Germany  
 Tel. (089) 32006-0  
 Telex 05-28282-0 eo d

Printed by Universitätsdruckerei  
 Dr. C. Wolf & Sohn  
 Heidemannstraße 166  
 8000 München 45  
 Fed. Rep. of Germany

¿ En todos los países existe la misma especie de vinchuca? No. Existen numerosas especies, aunque algunas son comunes para varios países de una misma región. En Chile existen solamente dos especies: una de hábitos domésticos llamada *Triatoma infestans* y otra de hábitos silvestres llamada *Triatoma spinolai*. Han sido encontradas en áreas rurales comprendidas entre los paralelos 18° y 34° de latitud Sur.

¿ Transmiten las vinchucas alguna enfermedad? Sí, la llamada enfermedad de Chagas o Trypanosomosis americana.

¿ Qué es la enfermedad de chagas? Es una enfermedad parasitaria producida por un protozoo llamado *Trypanosoma cruzi* el cual puede ser transmitido por vinchucas infectadas. La vinchuca no inyecta el parásito al picar. En algunas ocasiones, cuando la vinchuca ha succionado mucha sangre puede defecar y eliminar *T. cruzi* junto con la defecación. La defecación, que aparece como una gota líquida de color café oscuro, claramente visible, puede contaminar la herida de picadura, las pequeñas erosiones de la piel producidas por el rasquido o caer directamente en mucosa ocular, dando comienzo a la infección.

En la inmensa mayoría de los casos, la picadura de vinchuca no da lugar a ninguna infección, puesto que además de que no todas las vinchucas están infectadas, es necesario que éstas defequen en el momento de la picadura.

Cuando ocurre la infección, después de un período de incubación sin síntomas que dura aproximadamente 10 días, pueden aparecer manifestaciones que corresponden a la fase aguda de la enfermedad que se caracteriza por hinchazón a nivel del sitio de penetración del parásito, fiebre, malestar general y muy excep-

cionalmente puede haber miocarditis y/o meningitis. Al cabo de algunas semanas estas manifestaciones se atenúan y pueden desaparecer, dando lugar a una aparente curación espontánea de la infección.

A partir del sexto mes de ocurrida la infección inicial, la enfermedad entra en la fase crónica, que dura toda la vida de la persona y en la cual pueden aparecer manifestaciones correspondientes a compromiso miocárdico, del esófago o del colon.

En la mayoría de los casos, la infección es asintomática desde el comienzo.

¿ Pueden infectarse otros animales con el *Trypanosoma cruzi*? Sí. Especialmente los mamíferos terrestres, tanto silvestres como domésticos, los cuales pueden ser la fuente de infección de vinchucas domésticas o silvestres.

¿ Existe tratamiento para la enfermedad de Chagas? Sí. En la actualidad existen dos drogas, Nifurtimox y Benznidazol, de eficacia comprobada.

¿Cuál es la situación en La Silla? Existe en el área el *Triatoma spinolai*, especie silvestre, el cual atraído por el olor de las personas puede picarlas, especialmente mientras duermen.

El riesgo que infecten a las personas es escaso, porque han sido encontradas infectadas en una muy baja proporción (6,5%) y porque es necesario que defequen en el momento de la picadura.

¿ Qué precauciones hay que tomar? Mantener reparadas y utilizar adecuadamente las rejillas protectoras contra insectos de las ventanas de los dormitorios.

La administración de ESO está poniendo en práctica una serie de medidas técnicas destinadas a controlar y eliminar el problema de las vinchucas.

## Contents

Information on Vinchucas and Chagas Disease . . . . .	1
B. Reipurth: Star Formation in Bok Globules . . . . .	2
ESO Users Manual . . . . .	4
J. Danziger: X-Ray Surveys with the Einstein Observatory . . . . .	5
List of Preprints Published at the ESO Scientific Group . . . . .	6
R. P. Kudritzki, K. P. Simon and R. H. Méndez: The "Continuous" Central Stars of Planetary Nebulae – Are their Spectra Really Continuous? . . . . .	7
K. J. Fricke and W. Kollatschny: Variability of the Continuum and the Emission Lines in the Seyfert Galaxy Arakelian 120 . . . . .	9
Second ESO Infrared Workshop . . . . .	11
Y. and Y. Georgelin, A. Laval, G. Monnet and M. Rosado: Observations of the Giant Bubbles in the Large Magellanic Cloud . . . . .	11
G. Chincarini: Large-Scale Structures of the Universe . . . . .	14
B. Stolz: The Discovery of a New Su UMa Star . . . . .	16
P. Bouchet, Ch. Perrier, A. Brahic, J. Lecacheux and B. Sicardy: The Uranus Occultation of August 15, 1980 . . . . .	18
M. C. Lortet, G. Testor and L. Deharveng: RCW 58: A Remarkable HII Region Around a WN8 Star . . . . .	21
D. Enard: Installation and First Results of the Coudé Echelle Spectrometer . . . . .	22
D. Enard and M. Tarenghi: New Large Interference Filters for the 3.6-m Triplet . . . . .	24
Ch. Motch, S. A. Illovaisky and C. Chevalier: Discovery of a Very Fast Optical Activity in the X-Ray Source GX 339-4 . . . . .	28
Sonia (1967 – 1981) . . . . .	31
Personnel Movements . . . . .	31
Algunos Resúmenes . . . . .	31